NACA RM L51D19

NACA

RESEARCH MEMORANDUM

EFFECTS OF SPANWISE THICKNESS VARIATION ON THE AERODYNAMIC CHARACTERISTICS OF 35° AND 45° SWEPTBACK WINGS OF ASPECT RATIO 6

TRANSONIC-BUMP METHOD

By William D. Morrison, Jr., and Paul G. Fournier

Langley Aeronautical Laboratory
Langley Field, Va.

NATIONAL ADVISORY COMMITTEE FOR AERONAUTICS

WASHINGTON

July 10, 1951
Declassified August 31, 1954

NACA RM L51D19

NATIONAL ADVISORY COMMITTEE FOR AERONAUTICS

RESEARCH MEMORANDUM

EFFECTS OF SPANWISE THICKNESS VARIATION ON THE AERODYNAMIC CHARACTERISTICS OF 35° AND 45° SWEPTBACK WINGS OF ASPECT RATIO 6

TRANSONIC-BUMP METHOD

By William D. Morrison, Jr., and Paul G. Fournier

SUMMARY

An aerodynamic investigation has been conducted in the Langley high-speed 7- by 10-foot tunnel to determine the effects of taper-in-thickness on the aerodynamic characteristics of wings having 35° and 45° of sweepback, aspect ratio 6, and taper ratio 0.60. The wings were tapered from NACA 65A009 airfoil sections at the root chord to NACA 65A003 airfoil sections at the tip chord. The test Mach number range was from 0.60 to 1.14 at a Reynolds number of the order of 500,000.

The results of this investigation and comparisons with the results obtained from similar 35° and 45° sweptback wings of various constant section thickness ratios indicate that generally no sudden or undesirable variations in the aerodynamic characteristics can be expected in the transonic speed range for the wings of 6 percent thickness and wings tapered in thickness from 9 percent at the root to 3 percent at the tip. In addition, the tapered-in-thickness wings showed no evidence of large losses in lift-curve slope and forward movements in aerodynamic-center location at transonic speeds such as were found on the 9- and 12-percent constant-section-thickness-ratio wings of the same plan form. Agreement between experimental and theoretical lift slope and lateral center of pressure was generally good at subsonic speeds but fair to poor at low supersonic speeds. The comparisons between theoretical and experimental aerodynamic-center location were generally poor.

INTRODUCTION

Currently, appreciable interest is being shown in the design of comparatively high-aspect-ratio sweptback wings for use on bomber-type aircraft wich might cruise at high subsonic speeds but be capable of flight at low supersonic speeds. The design of a wing for such an aircraft would of necessity be a compromise between structural and aerodynamic considerations. Data previously obtained from wings of constant section thickness ratios practical for the design of the aforementioned-type aircraft have shown undesirable static stability characteristics at transonic speeds (references 1 and 2) caused by loss of the tip load. It was thought that tapering the thickness ratio of these sweptback wings would enable the designer to obtain the desired structural qualities but retain tip sections thin enough to eliminate or minimize the loss in tip load.

Accordingly, an investigation has been conducted in the Langley high-speed 7- by 10-foot tunnel to determine the aerodynamic characteristics of tapered-in-thickness wings with 35° and 45° of sweepback, aspect ratio 6, and taper ratio 0.60. These wings were tapered in thickness by straight-line elements from NACA 65A009 airfoil sections at the root chord to NACA 65A003 airfoil sections at the tip chord. A modified transonic bump was used which enabled a Mach number range from 0.60 to 1.15 to be obtained.

The purpose of this paper is to present the experimental results of this investigation of the tapered-in-thickness wings and to analyze those data in light of information available from previous investigations (references 1, 3, and 4 and unpublished data) of wings with the same plan forms but with different constant section thickness ratios. Comparisons are also made with theoretical values at subsonic and low supersonic speeds.

COEFFICIENTS AND SYMBOLS

All the force and moment data presented are referred to the wind axes. Pertinent symbols are defined as follows:

C_L lift coefficient (Twice semispan lift/qS)

C_D drag coefficient (Twice semispan drag/qS)

C_m pitching-moment coefficient referred to $0.25\bar{c}$ (Twice semispan pitching moment/$qS\bar{c}$)

C_B bending-moment coefficient due to lift about wing root $\left(\text{Root bending moment}/q\,\frac{S}{2}\,\frac{b}{2}\right)$

ΔC_D drag coefficient due to lift $\left(C_D - C_{D_{min}}\right)$

c_l section lift coefficient

q effective dynamic pressure over span of model, pounds per square foot $\left(\frac{1}{2}\rho V^2\right)$

ρ mass density of air, slugs per cubic foot

V free-stream velocity, feet per second

S twice wing area of semispan model, square feet

$\bar{c}$ mean aerodynamic chord of wing using theoretical tip, feet $\left(\frac{2}{S}\int_0^{b/2} c^2 dy\right)$

c local wing chord, feet

c_{av} average wing chord, feet

b twice span of semispan model, feet

$\frac{t}{c}$ airfoil-section thickness ratio, percent

t maximum local-wing-chord thickness, feet

E modulus of elasticity in bending, pounds per square inch

y spanwise distance from plane of symmetry, feet

d chordwise distance from leading edge of root chord to wing aerodynamic center, feet

l chordwise distance from leading edge of root chord to quarter-chord point of mean aerodynamic chord, feet

$\frac{cc_l}{C_L c_{av}}$ span-load coefficient (reference 2)

M effective Mach number over span of model

M_a average chordwise Mach number

M_l local Mach number

y_{c_p} lateral center of pressure, percent semispan $\left(100 \frac{C_B}{C_L}\right)$

α angle of attack, degrees

α_D local angle of streamwise twist, degrees

$\frac{\alpha_D}{qC_L}$ local twist parameter

Λ angle of sweepback relative to quarter-chord line, degrees

$\Delta\Lambda$ incremental angle of sweepback due to flow angularity over bump surface, degrees

MODELS AND METHODS

Wing Geometry

The steel-wing semispan models had 35° and 45° of sweepback referred to the quarter-chord line, aspect ratio 6, taper ratio 0.60, and NACA 65A009 airfoil sections at the root chord measured parallel to the free stream tapered in thickness by straight-line elements to NACA 65A003 airfoil sections at the tip chord. Details of the model geometry are shown in figure 1 and a photograph of a typical test setup is given as figure 2. The variation of wing thickness ratio along the semispan is presented in figure 3.

Modified Transonic Bump

The subject wings were tested on a modified version of the original transonic bump. Typical Mach number contours over the test section of the modified transonic bump are shown in figure 4. Effective Mach numbers

were obtained from charts similar to those of figure 4 using the relationship:

$$M = \frac{2}{S}\int_0^{b/2} cM_a \, dy$$

The bump boundary-layer thickness was such that 95 percent of the free-stream velocity was reached at a distance of approximately 0.25 inch measured at the balance center line; this represents a value of 4.8 percent of the semispan of the models tested.

Surveys over the bump in the region of the test section (fig. 4) showed less than 0.03 spanwise Mach number gradient at the lower Mach numbers. This gradient increased to approximately 0.05 at the highest test Mach numbers. Chordwise gradients were not appreciable for Mach numbers below unity. Above Mach number of 1.00 the chordwise gradient was about 0.01.

The variation of average Reynolds number, based on $\bar{c}$, with Mach number is presented in figure 5.

In order to eliminate the use of end plates and the subsequent difficulty in determining end-plate corrections, a turntable was used on the modified transonic bump. This turntable was flush with the bump surface and supported so as to retain the contour of the bump at all angles of attack. Cutouts slightly larger than the wing-root sections were made in the bump turntable through which the wings projected. In order to minimize leakage from inside the bump, a sponge seal was attached to the wing butt in such a manner that it wiped against the inside of the turntable.

Comparisons of Modified and Original Transonic Bumps

The wings of similar plan form with which the subject wings are compared were tested on the original transonic bump. A comparative scaled drawing of the original and modified transonic bump is presented in figure 6. Figure 7 shows Mach number contours over the test section of both bumps with models in place at a representative Mach number of approximately 1.00. It can be seen that the gradient over the span of the model located on the modified bump is about half as large as on the original bump; the chordwise gradient being about the same.

It should be noted that the flow curvature over the bump surface produces an effective variation in the sweep angle along the span. This variation of $\Delta\Lambda$ (fig. 7) is presented only along the bump surface inasmuch as it has been found that the streamlines over the bump are

essentially parallel. The short vertical lines seen in this plot represent a projection of the limits of the quarter-chord lines of the 35° and 45° sweptback wings with models in the test locations. It can also be seen from figure 7 that the local flow curvature is also reduced by about half on the modified bump. Unfortunately, however, the boundary-layer thickness is almost doubled on the modified bump.

Comparisons of data obtained on similar wings tested on the two transonic bumps and also on a reflection plane setup (which essentially eliminates flow curvature and Mach number gradients) indicated no large or consistent differences in the results obtained from the different techniques (unpublished data). Therefore, it is believed that the trends of the results presented in this paper should not be appreciably affected by the differences in the flow curvature and Mach number gradients present on the two bumps. A discussion of many of the factors that must be considered in evaluating the bump test results can be found in reference 5.

Corrections

The restricted size of the bump turntable necessitated mounting the 45° sweptback wing 40 percent ahead of the desired quarter-chord point of the mean aerodynamic chord. Consequently, a 40-percent $\bar{c}$ transfer to the pitching-moment data of this wing was applied.

In view of the small size of the models relative to the effective flow field, jet-boundary and blockage corrections were believed to be insignificant and hence were not applied.

In order to determine the aeroelastic properties of the wings used in the analysis of this paper, concentrated static loads were applied to the various wings at the two spanwise locations on the quarter-chord lines shown in figure 8, and the variation of the angle of streamwise twist was measured at four spanwise locations. (See fig. 8.) These loads were applied so as to simulate theoretical span loadings. The variations of angle of streamwise twist along the model spans were used to correct rigid theoretical aerodynamic parameters to an elastic condition.

THEORETICAL CONSIDERATIONS

Incompressible aerodynamic characteristics were calculated by the discrete vortex method of reference 6. The lateral center-of-pressure and

aerodynamic-center locations were assumed to be invarient at subcritical speeds, but the lift slopes were corrected for compressibility by use of the charts of reference 7. Aerodynamic characteristics at low supersonic speeds were determined using the linearized theory of references 8 and 9. All the theoretical parameters were corrected by strip-theory methods to an elastic condition using the values of streamwise twist shown in figure 8. The equations used for these corrections are summarized as follows:

$$C_{L_\alpha} = C_{L_\alpha}' \int_0^1 \left[1 + \left(\frac{\alpha_D}{qC_L} \right) qC_{L_\alpha}' \right] \frac{cc_l}{C_L c_{av}} d\left(\frac{y}{\frac{b}{2}} \right)$$

$$y_{c_p} = \frac{C_{L_\alpha}'}{C_{L_\alpha}} \int_0^1 \left[1 + \left(\frac{\alpha_D}{qC_L} \right) qC_{L_\alpha}' \right] \frac{cc_l}{C_L c_{av}} \frac{y}{\frac{b}{2}} d\left(\frac{y}{\frac{b}{2}} \right)$$

$$\frac{\partial C_m}{\partial C_L} = \frac{l - d}{\bar{c}}$$

$$\frac{d}{\bar{c}} = \frac{C_{L_\alpha}'}{C_{L_\alpha}} \int_0^1 \left[1 + \left(\frac{\alpha_D}{qC_L} \right) qC_{L_\alpha}' \right] \frac{cc_l}{C_L c_{av}} \frac{x}{\bar{c}} d\left(\frac{y}{\frac{b}{2}} \right)$$

where

C_{L_α}' theoretical rigid lift-curve slope

C_{L_α} theoretical elastic lift-curve slope

x distance from root leading edge to local quarter-chord (subsonic) or to local aerodynamic center (supersonic), feet

The remainder of the symbols have been previously defined.

RESULTS AND DISCUSSION

Presentation of Results

Results of this investigation are presented in the following figures. Slopes presented in the summary figures were measured through zero lift up to a lift coefficient where obvious departures from linearity occurred.

Characteristics of 45° Sweptback Wings

Lift characteristics.- Perhaps the most significant effect of thickness on the lift characteristics is observed in the Mach range between 0.90 and 1.10. (See figs. 10 and 11(a).) In this speed range large reductions in $\partial C_L/\partial \alpha$ in the low lift range were evident for wings having wing-tip thickness ratios of 9 and 12 percent. It can be seen from the curves of lateral center of pressure that most of this lift loss must occur over the outboard wing sections. (See fig. 10.) Utilization of wings with outboard wing sections of 6 percent or less markedly reduced or eliminated the undesirable lift characteristics at transonic speeds. The differences in the absolute values of lift slope for the thickness series at a given subsonic speed (fig. 10) are largely attributable to differences in aeroelastic effects as can be seen from the

generally good agreement between the elastic theoretical values of lift slope and experiment (fig. 12). For Mach numbers greater than 1.10, however, the theoretical values are considerably higher than the corresponding experimental slopes.

Study of the lateral center-of-pressure variations with Mach number (fig. 10) clearly indicates that even at the highest test Mach number of 1.14 the loss in lift on the outboard sections of the thicker wings is not recovered, hence, resultant poor agreement with theory.

Drag characteristics.- It should be pointed out that the magnitude of drag coefficients shown in figure 10 may be affected somewhat by the low Reynolds number of these tests (that is, larger differences in $C_{D_{min}}$ against t/c have been obtained on some airfoil sections in the range of the present test Reynolds numbers than at the much higher Reynolds number of flight. (See reference 10.)) However, the variations of $C_{D_{min}}$ with Mach number are believed to be valid. One of the most noteworthy things pertaining to the minimum drag characteristics of this family of wings is the surprisingly low drag indicated at the highest test Mach numbers for the tapered-in-thickness wing. If it is assumed that the pressure drag at supersonic speeds is approximately proportional to the $\left(\frac{t}{c}\right)^2$, then the effective thickness of this wing is about 6.9 percent; nevertheless, it showed about the same drag at $M = 1.14$ as the comparable wing with 6-percent-thick sections. (See fig. 10.)

The variation of pressure drag at zero lift with $\left(\frac{t}{c}\right)^2$ at $M = 1.15$ is presented in figure 13. The wing of 6-percent constant thickness shows somewhat higher drag than might be expected with a linear variation of pressure drag with $\left(\frac{t}{c}\right)^2$; whereas the tapered-in-thickness wing had slightly less drag than was estimated.

No consistent trends were observed in the drag-due-to-lift parameter (fig. 11(b)). At the lowest comparative Mach number, $M = 0.80$, the 12-percent-thick wing shows considerably less ΔC_D than the thinner wings, mainly because of greater leading-edge suction. The peculiar variation of drag due to lift at $M = 1.00$ for the thicker wing is a result of the nonlinear lift characteristics coupled with loss of leading-edge suction.

Pitching-moment characteristics.- As a result of the previously noted large losses in lift over the outer portions of the 12- and 9-percent-thick wings, extremely large forward shifts in aerodynamic

center $\left(\text{positive values of } \frac{\partial C_m}{\partial C_L}\right)$ are produced at transonic speeds. (See fig. 10.) Although it could be reasoned that any large stability changes produced might occur at lower lift coefficients than would be encountered in normal flight conditions, undesirable variations of stick position and control force with Mach number might be produced when accelerating through the transonic speed range. For the two wings of the least thickness no objectionable trends are observed in the lower lift range at transonic speeds. It can be seen that the aerodynamic-center location of the 6-percent and 9- to 3-percent-thick wings are from 12 to 16 percent behind the theoretical imcompressible aerodynamic-center location corrected for aeroelasticity. (See fig. 12.) Inasmuch as the lateral center of load is in good agreement with theory, it is believed that most of the disparity between theory and experiment must be caused by a rearward movement of the chordwise center of pressure, perhaps as a result of vortex-type flow. Apparently sizeable scale effects are present, since a wing geometrically similar to the 6-percent-thick wing, tested at low speed and high Reynolds number, has been found to have an aerodynamic-center location near the theoretical value. At supersonic speeds, agreement between theory and experiment is generally poor. For reasons previously discussed, the thicker wings have aerodynamic-center locations appreciably ahead of the theoretical values; whereas the wing with the thinnest tip (tapered 9 to 3) shows an aerodynamic-center location considerably behind the theoretically determined location (fig. 12).

The pitching-moment characteristics at higher lifts (fig. 11(c)) indicate that at Mach numbers up to and above 1.00, a severe unstable trend is evident above $C_L = 0.4$ on the tapered 9 to 3 percent wing. At the highest Mach numbers, this tendency is delayed to a somewhat higher lift coefficient and the severity of the instability is reduced. It is difficult to compare these higher lift characteristics with those of the other wings because of the limited lift range obtained for the comparison wings.

Characteristics of 35° Sweptback Wings

Lift characteristics.- Subcritically the lift-curve slope measured near zero lift for the tapered 9 to 3 percent wing shows approximately a 10 percent increase over the constant 6-percent-thick wing (fig. 15) which is chiefly attributable to the greater stiffness of the former wing, as seen from figure 8. Although the variation of lift slope with Mach number for the two wings is somewhat different, no sudden losses in lift through the transonic speed range are experienced. Theoretical values of lift-curve slope against Mach number (fig. 17) for both the tapered 9- to 3-percent and constant 6-percent-thick wings are somewhat

lower than experimental values at subcritical Mach numbers, but at low supersonic Mach numbers, the theoretical values are considerably higher than the experimental results. Theoretical values of lateral center of pressure (fig. 17) for both wing configurations are in fairly good agreement with experiment at all Mach numbers investigated.

Drag characteristics.- The values of the minimum drag coefficient (fig. 15) throughout the test Mach number range were approximately 0.003 higher for the tapered 9 to 3 percent wing than for the constant 6-percent-thick wing. Drag rise for both configurations occurred at a Mach number of about 0.93. At Mach number 0.80, and at a moderate lift coefficient of 0.4, no difference is shown in the drag due to lift (fig. 16(b)) for the two wings. However, at $M = 0.95$, the tapered-in-thickness wing has somewhat higher drag above a lift coefficient of 0.5, principally because of indications of an earlier onset of stall.

Pitching-moment characteristics.- The data for the tapered-in-thickness wing indicate slightly less change in wing aerodynamic-center location with Mach number than for the constant thickness wing; however, an unstable pitching-moment tendency is seen to occur at a somewhat lower lift coefficient at subsonic speeds for the wing with the thinner tip. (See figs. 15 and 16(c).) No sudden movement in aerodynamic-center location was shown for these wings through the transonic speed range. The theoretical aerodynamic-center locations are from 5 to 10 percent of the mean aerodynamic chord forward of the experimental values at subsonic Mach numbers. (See fig. 17.) Inasmuch as the experimental lateral center-of-pressure locations are in fairly good agreement with theory (fig. 17), it is probable that the discrepancy between the theoretical and experimental aerodynamic centers may be caused by a chordwise shift in center of pressure as previously discussed under the 45° wing series. At the low supersonic Mach numbers, agreement between theory and experiment is fairly good.

CONCLUDING REMARKS

The results of an investigation to determine the effects of thickness changes on the characteristics of a series of 35° and 45° sweptback wings have indicated that no sudden or undesirable variations in the aerodynamic characteristics can be expected in the transonic speed range for the wings of 6 percent thickness and wings tapered in thickness from 9 percent at the root to 3 percent at the tip. In addition, the tapered-in-thickness wings showed no evidence of large loss in lift-curve slope and forward movements in aerodynamic-center location at transonic speeds

such as were found on the 9- and 12-percent constant-section-thickness-ratio wings of the same plan form. Agreement between experimental and theoretical lift slope and lateral center of pressure was generally good at subsonic speeds but fair to poor at low supersonic speeds. The comparisons between theoretical and experimental aerodynamic-center location were generally poor.

Langley Aeronautical Laboratory
National Advisory Committee for Aeronautics
Langley Field, Va.

REFERENCES

1. Polhamus, Edward C., and King, Thomas J.: Aerodynamic Characteristics of Tapered Wings Having Aspect Ratios of 4, 6, and 8, Quarter-Chord Lines Swept Back 45° and NACA 63_1A012 Airfoil Sections. Transonic-Bump Method. NACA RM L51C26, 1951.

2. Campbell, George S., and Morrison, William D., Jr.: A Small-Scale Investigation of "M" and "W" Wings at Transonic Speeds. NACA RM L50H25a, 1950.

3. Goodson, Kenneth W., and Few, Albert G., Jr.: Aerodynamic Characteristics of a Wing with Quarter-Chord Line Swept Back 45°, Aspect Ratio 6, Taper Ratio 0.6, and NACA 65A006 Airfoil Section. Transonic-Bump Method. NACA RM L9I08, 1949.

4. Sleeman, William C., Jr., and Morrison, William D., Jr.: Aerodynamic Characteristics of a Wing with Quarter-Chord Line Swept Back 35°, Aspect Ratio 6, Taper Ratio 0.6, and NACA 65A006 Airfoil Section. Transonic-Bump Method. NACA RM L9K10a, 1949.

5. Donlan, Charles J., and Myers, Boyd C., II, Mattson, Axel T.: A Comparison of the Aerodynamic Characteristics at Transonic Speeds of Four Wing-Fuselage Configurations as Determined from Different Test Techniques. NACA RM L50H02, 1950.

6. Campbell, George S.: A Finite-Step Method for the Calculation of Span Loadings of Unusual Plan Forms. NACA RM L50L13, 1951.

7. DeYoung, John: Theoretical Additional Span Loading Characteristics of Wings with Arbitrary Sweep, Aspect Ratio, and Taper Ratio. NACA TN 1491, 1947.

8. Cohen, Doris: Theoretical Loading at Supersonic Speeds of Flat Swept-Back Wings with Interacting Trailing and Leading Edges. NACA TN 1991, 1949.

9. Malvestuto, Frank S., Jr., Margolis, Kenneth, and Ribner, Herbert S.: Theoretical Lift and Damping in Roll at Supersonic Speeds of Thin Sweptback Tapered Wings with Streamwise Tips, Subsonic Leading Edges, and Supersonic Trailing Edges. NACA Rep. 970, 1949. (Formerly NACA TN 1860.)

10. Jacobs, Eastman N., and Sherman, Albert: Airfoil Section Characteristics as Affected by Variations of the Reynolds Number. NACA Rep. 586, 1937.

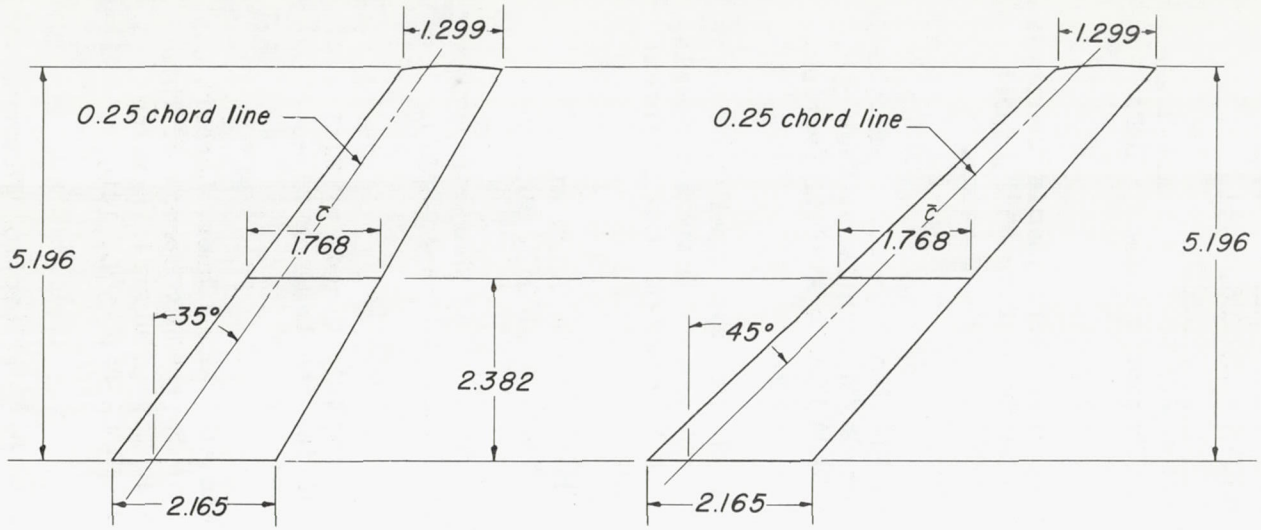

Tabulated Wing Data

Area (twice semispan)	0.125 sq ft
Aspect ratio	6.0
Taper ratio	0.6
Airfoil section parallel to free stream	NACA 65A009 at root chord to NACA 65A003 at tip chord

NACA

0 1 2

Scale, inches

Figure 1.- Plan-form drawing of wings having 35° and 45° of sweepback, aspect ratio 6, taper ratio 0.6, and NACA 65A009 airfoil section at root chord tapered to NACA 65A003 airfoil section at tip chord.

Figure 2.- Photograph of a model on the modified transonic bump.

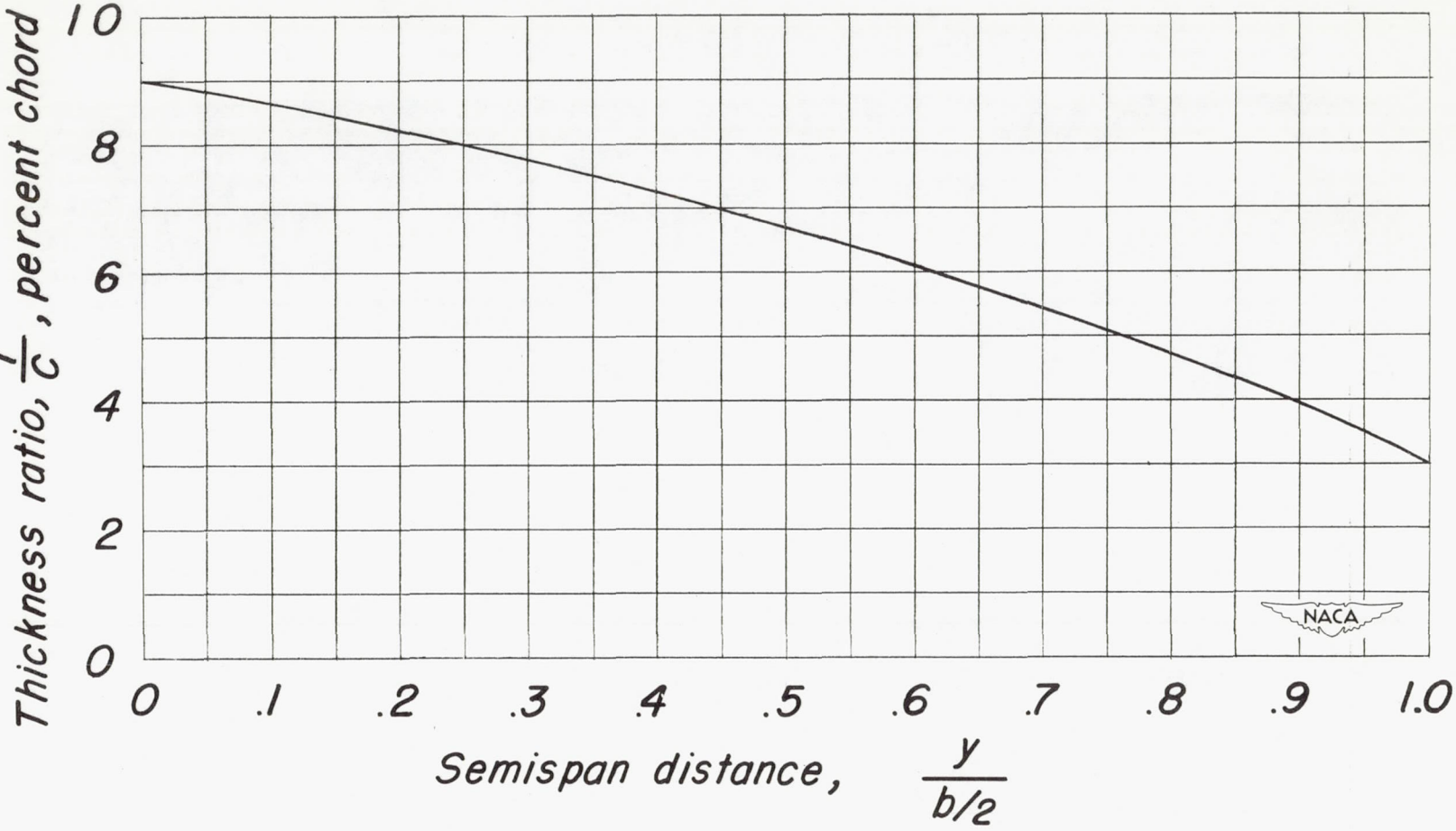

Figure 3.- Thickness ratio distribution along span of models having 35° and 45° of sweepback, aspect ratio 6, taper ratio 0.6, and NACA 65A009 airfoil sections at the root chord tapered to NACA 65A003 airfoil sections at the tip section.

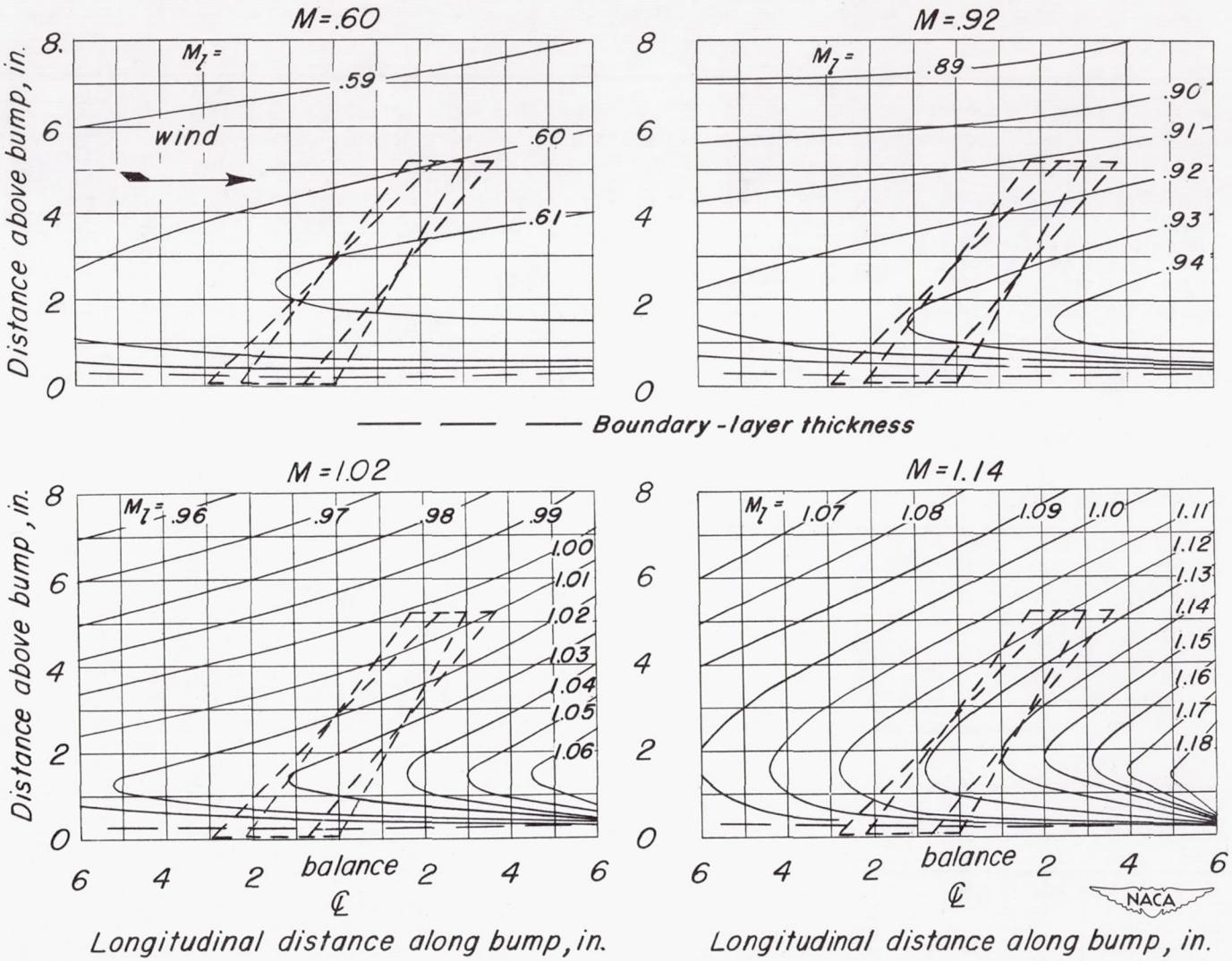

Figure 4.- Typical Mach number contours in vicinity of model on modified transonic bump.

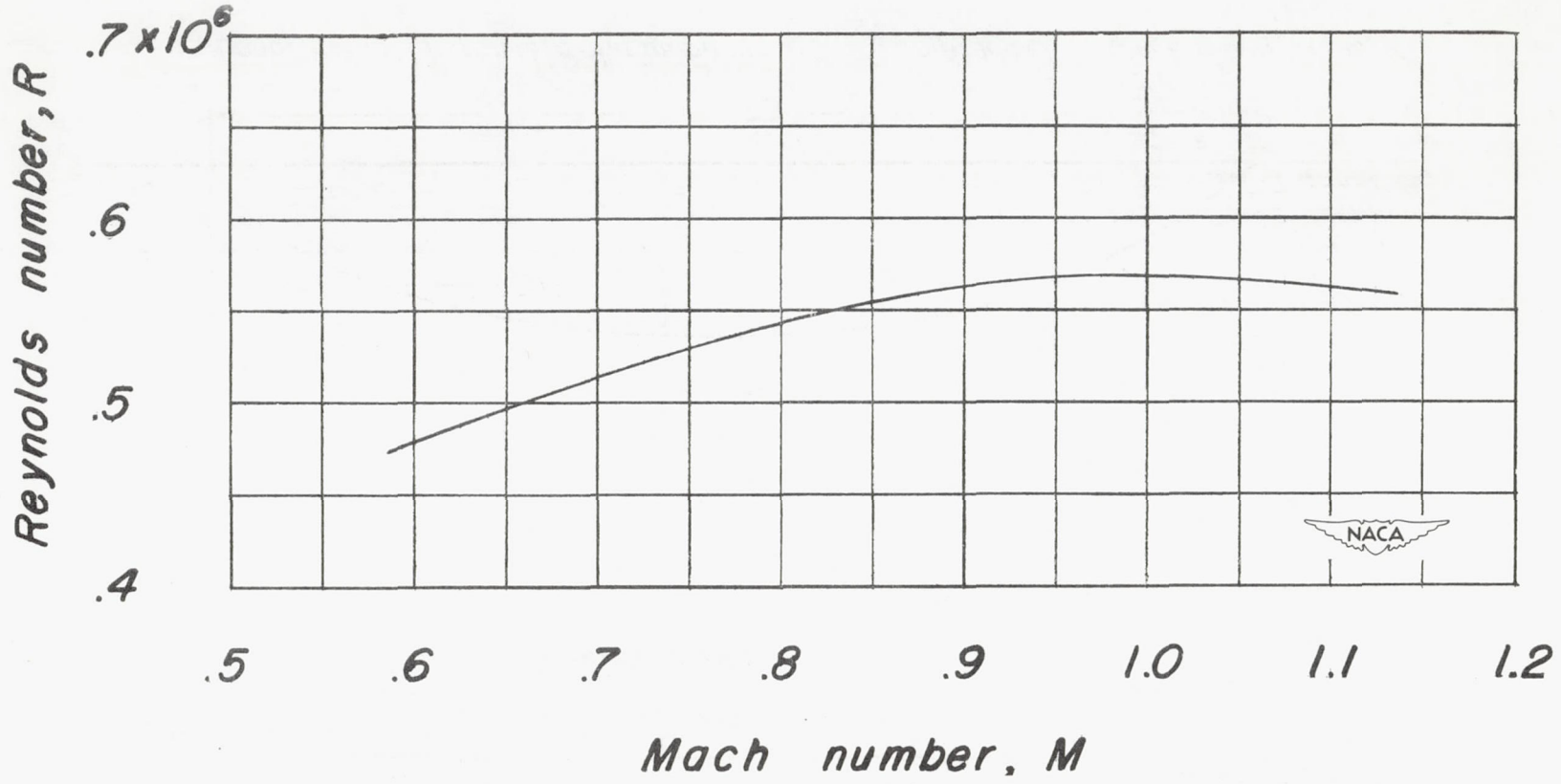

Figure 5.- Variation of average test Reynolds number with Mach number for wings having 35° and 45° of sweepback, aspect ratio 6, taper ratio 0.6, and NACA 65A009 airfoil sections at the root chord tapered to NACA 65A003 airfoil sections at the tip chord.

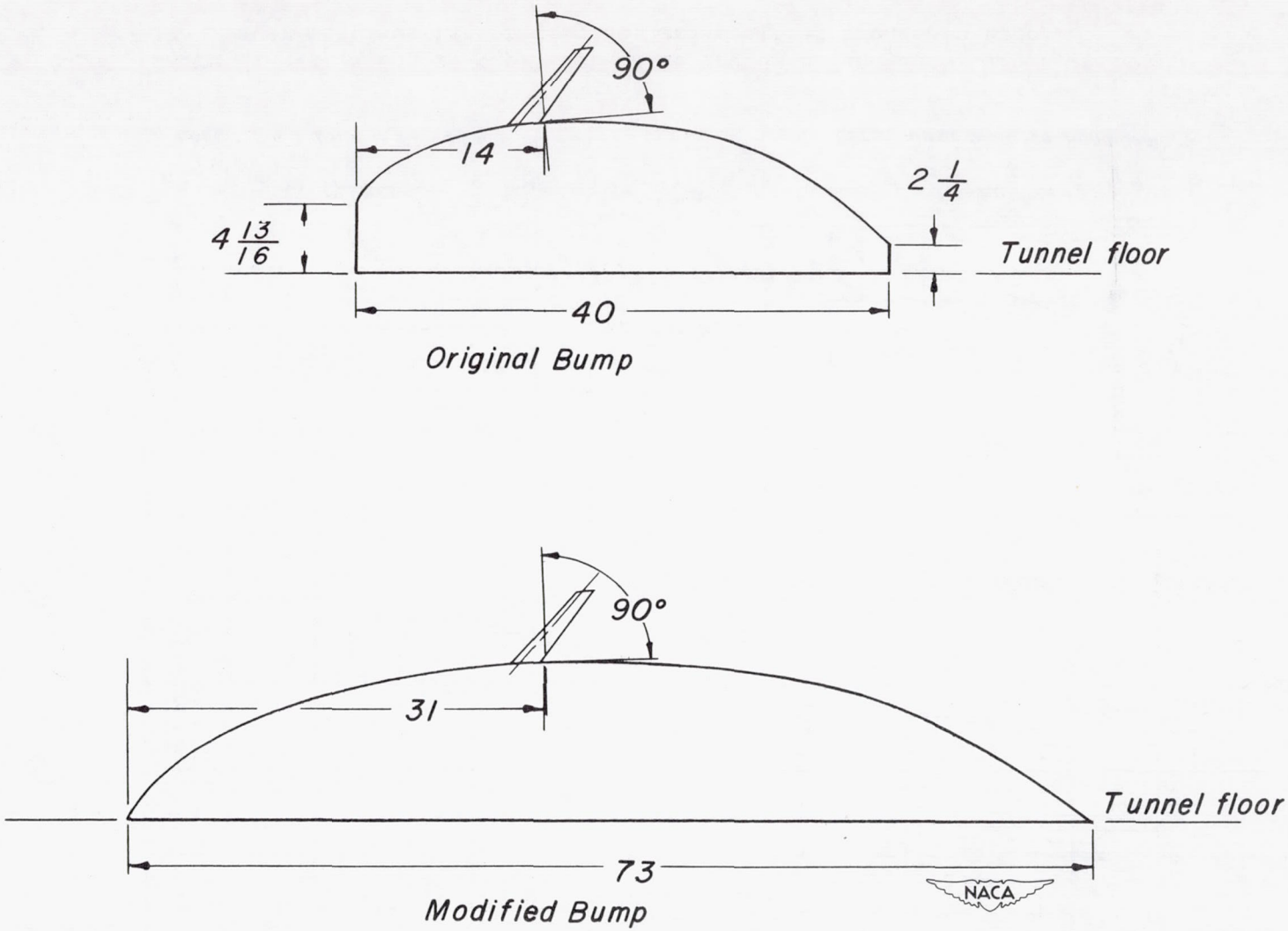

Figure 6.- Comparative scaled drawing of original and modified transonic bumps.

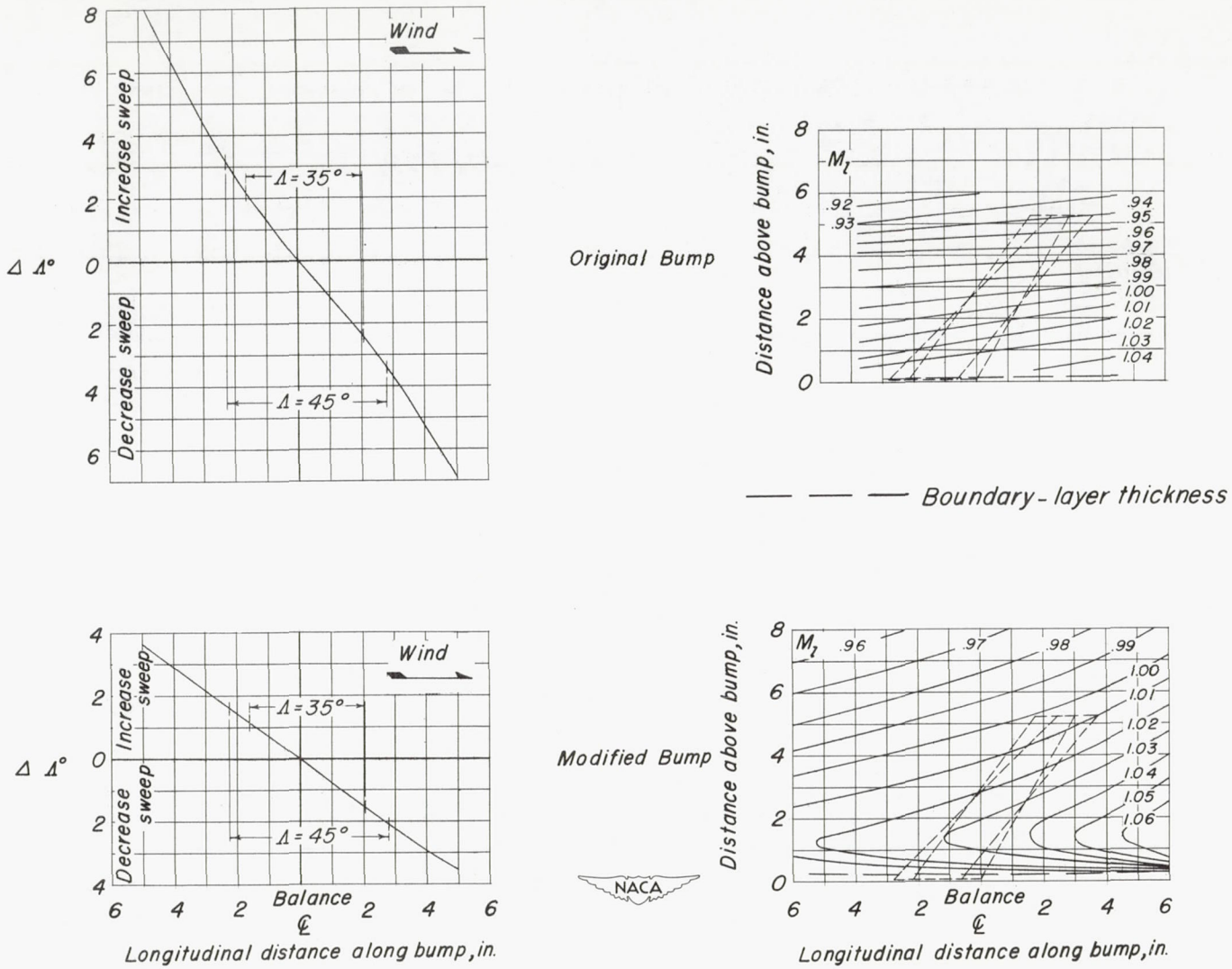

Figure 7.- Variation of the sweep-angle increment and Mach number gradients over test section of original and modified transonic bumps.

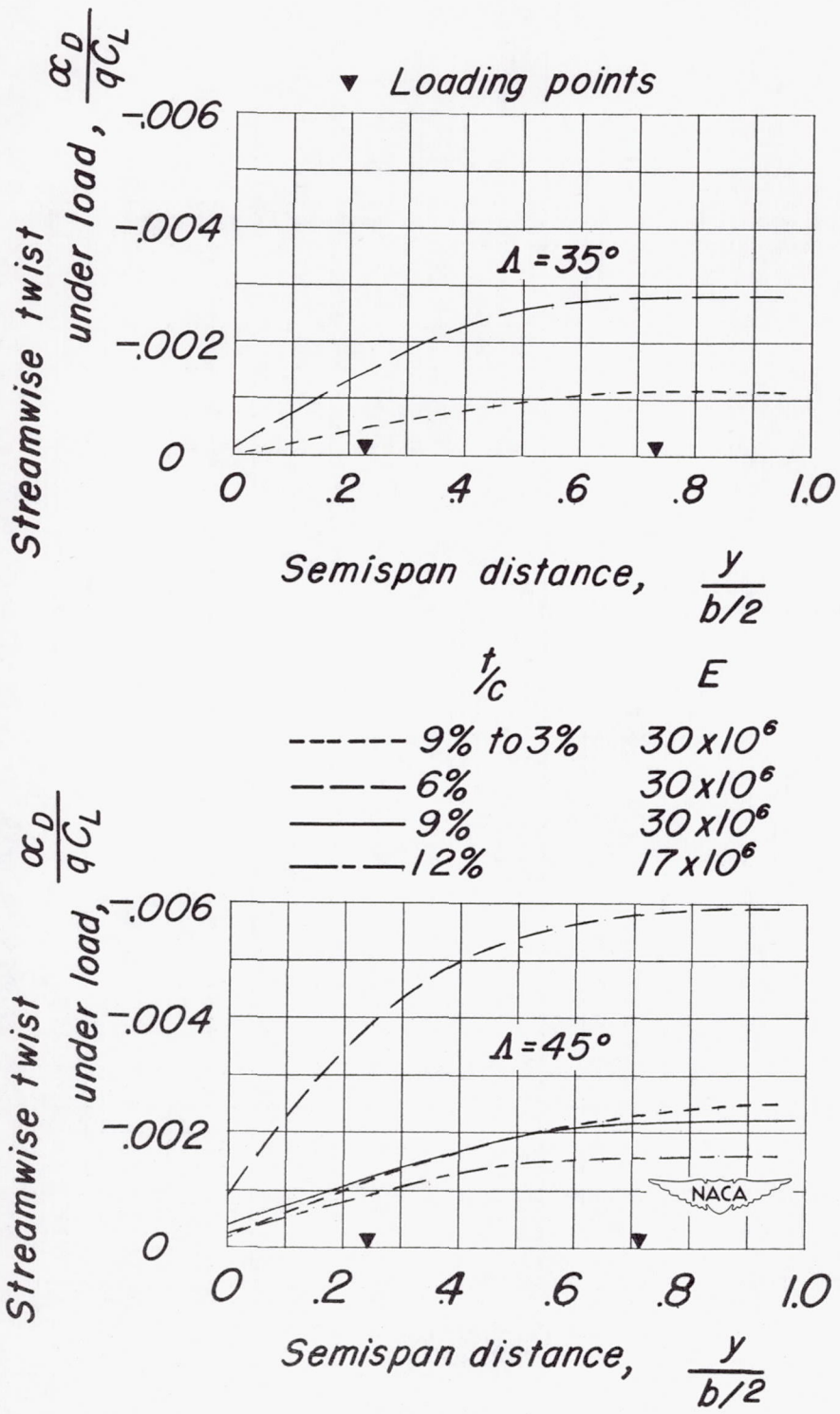

Figure 8.- Effect of thickness on variation of angle of streamwise twist along model span for wings having 35° and 45° of sweepback, aspect ratio 6, and taper ratio 0.6.

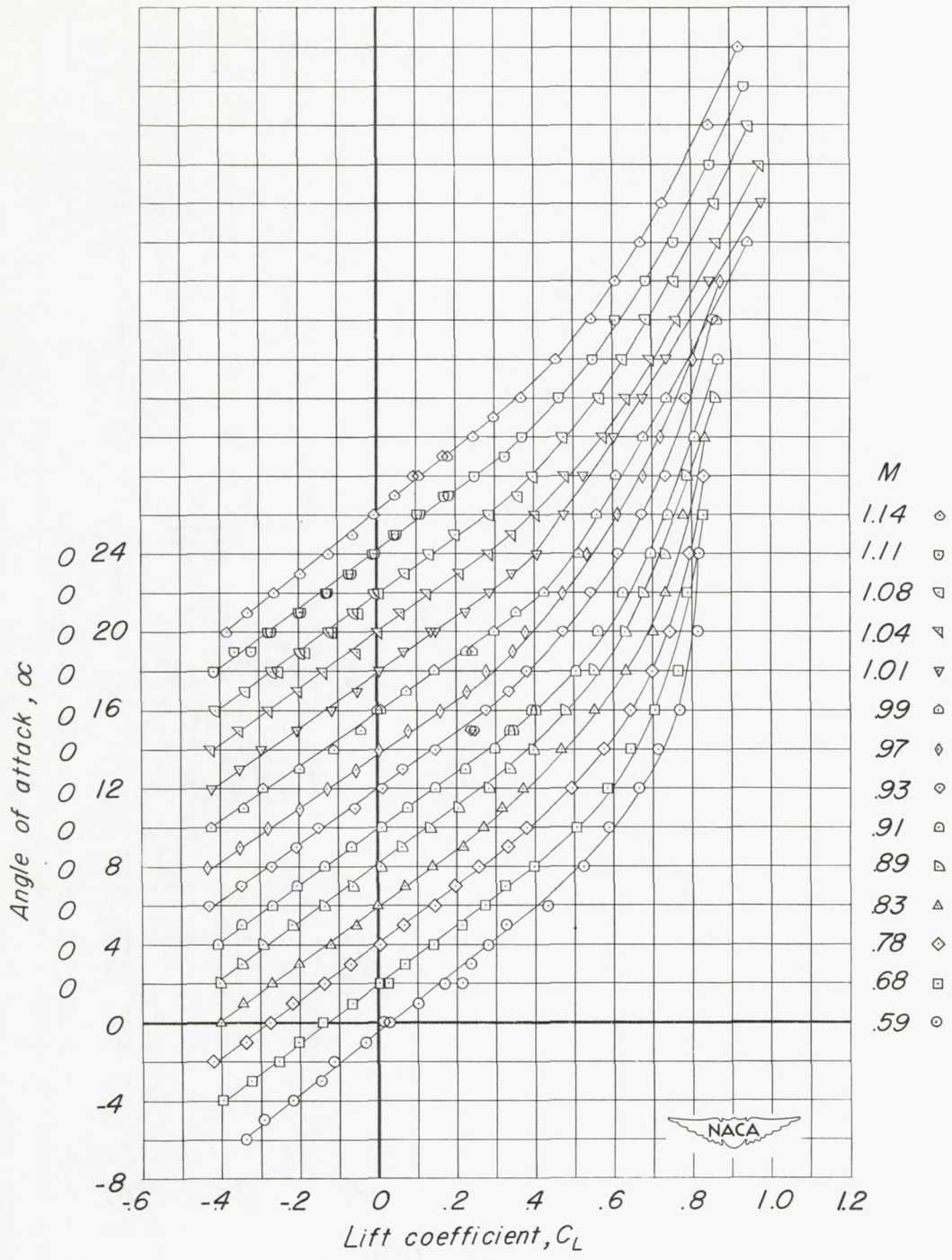

(a) α against C_L.

Figure 9.- Basic aerodynamic data for a wing having 45° of sweepback, aspect ratio 6, taper ratio 0.6, and NACA 65A009 airfoil section at the root chord tapered to NACA 65A003 airfoil section at tip chord.

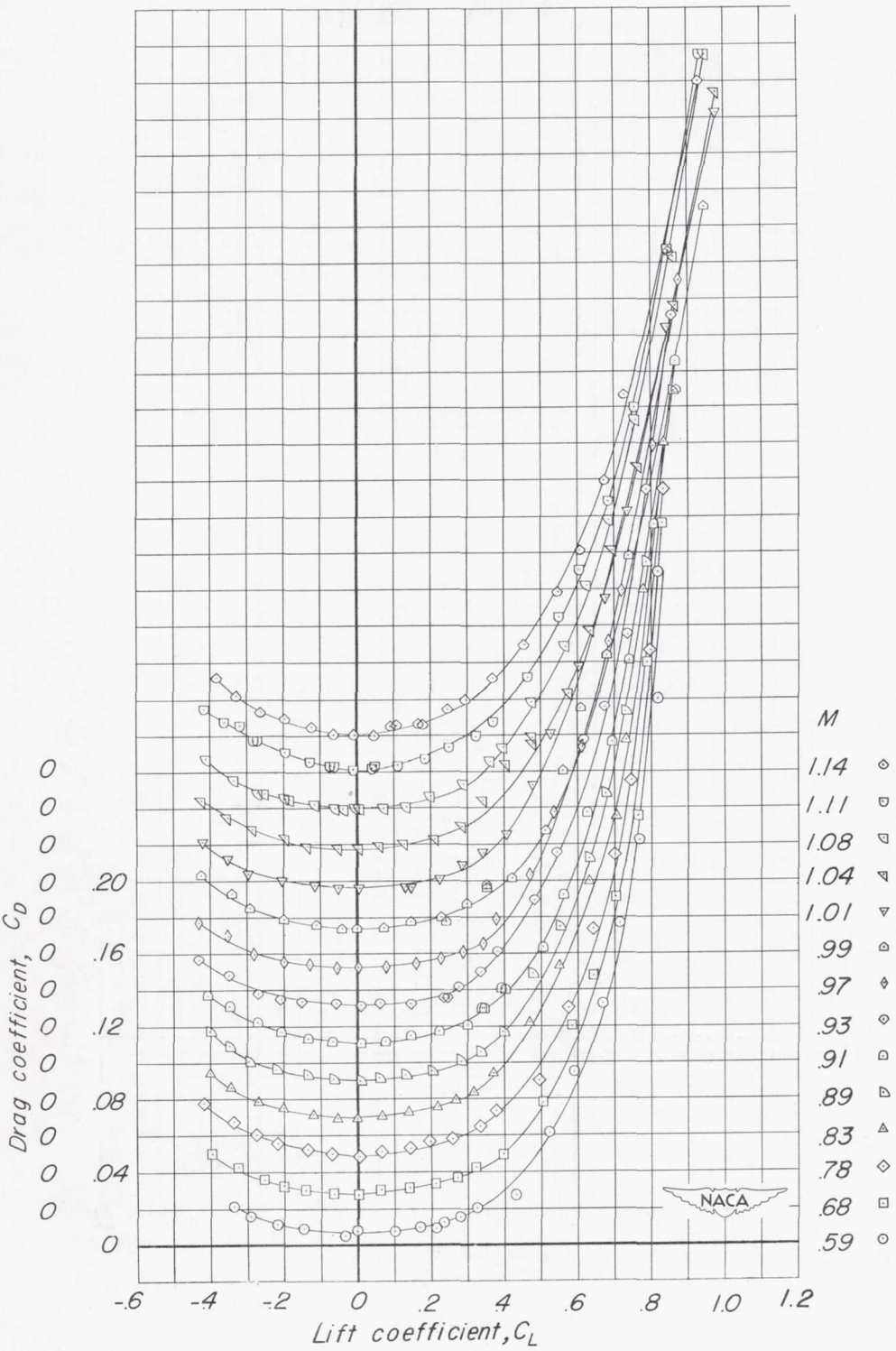

(b) C_D against C_L.

Figure 9.- Continued.

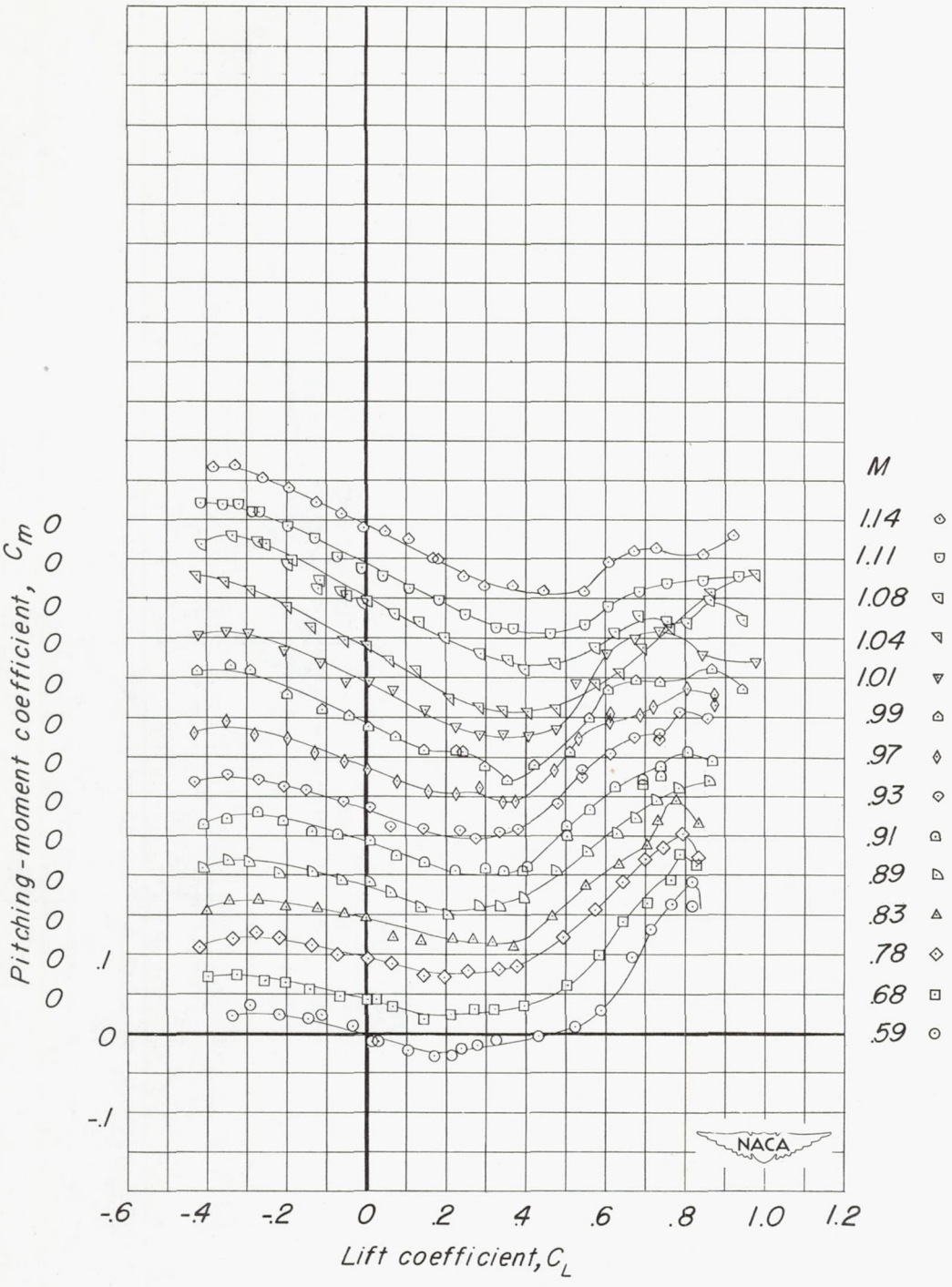

(c) C_m against C_L.

Figure 9.- Continued.

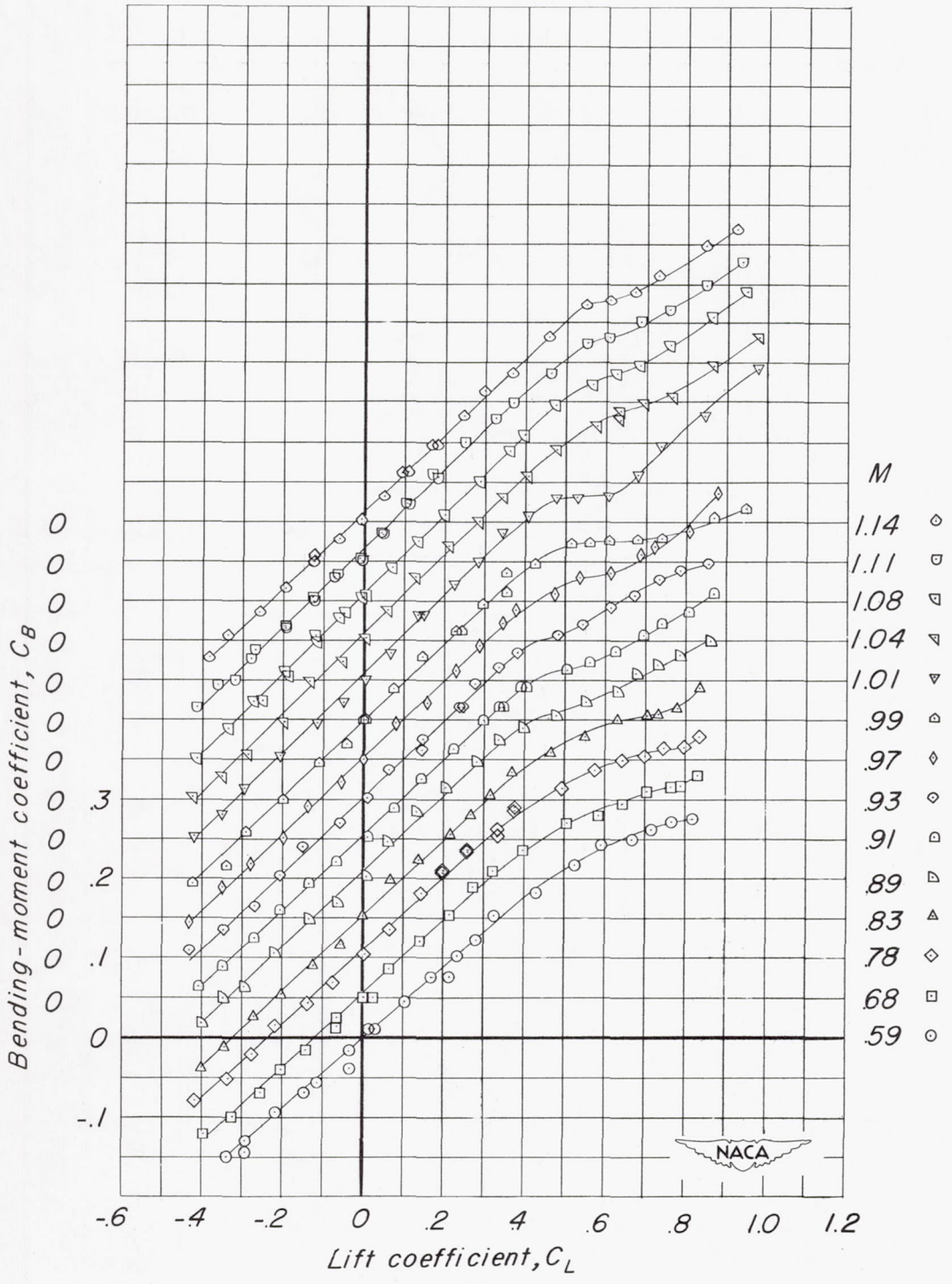

(d) C_B against C_L.

Figure 9.- Concluded.

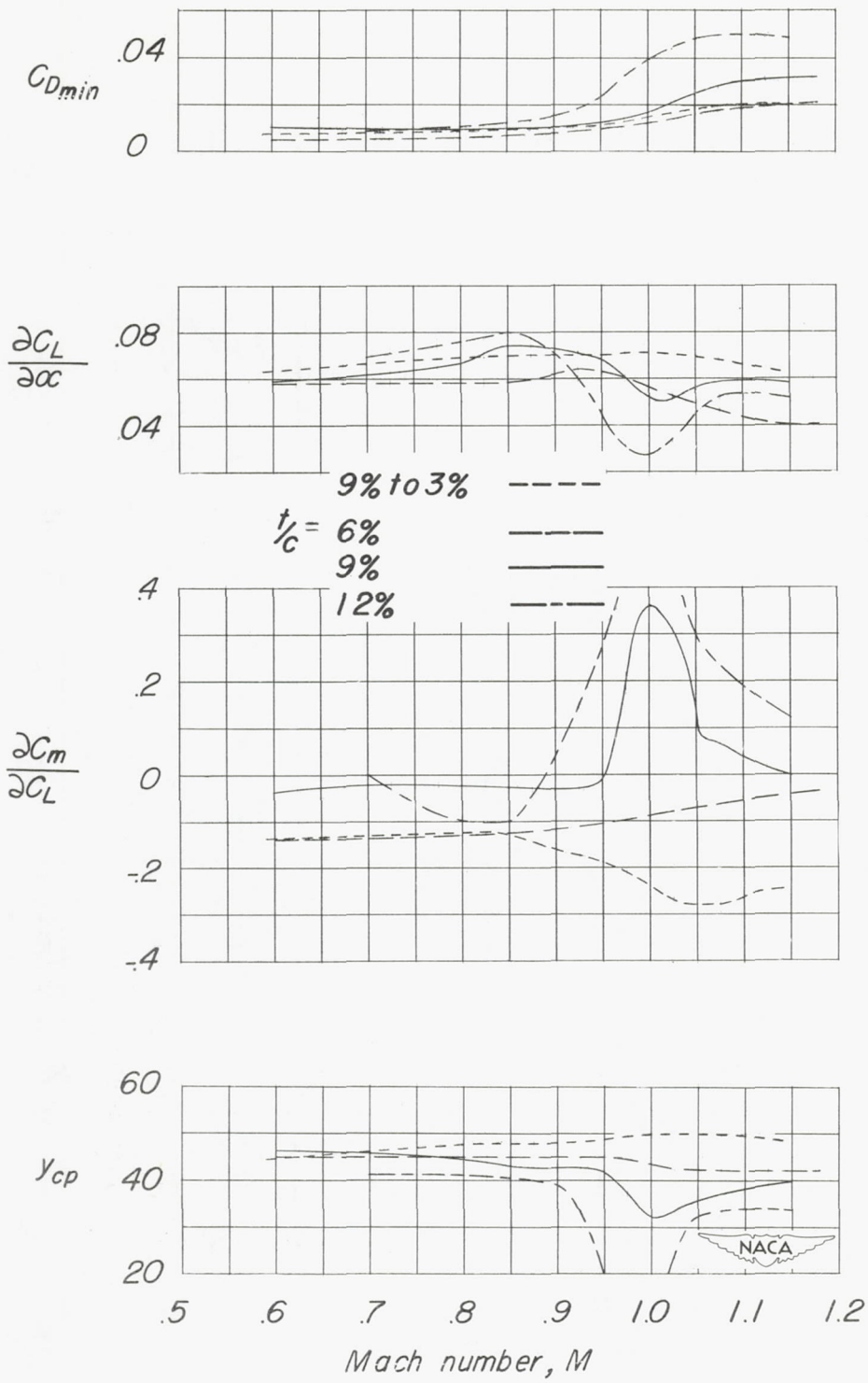

Figure 10.- Comparison of the effects of thickness ratio on the aerodynamic characteristics of wings having 45° of sweepback, aspect ratio 6, and taper ratio 0.6.

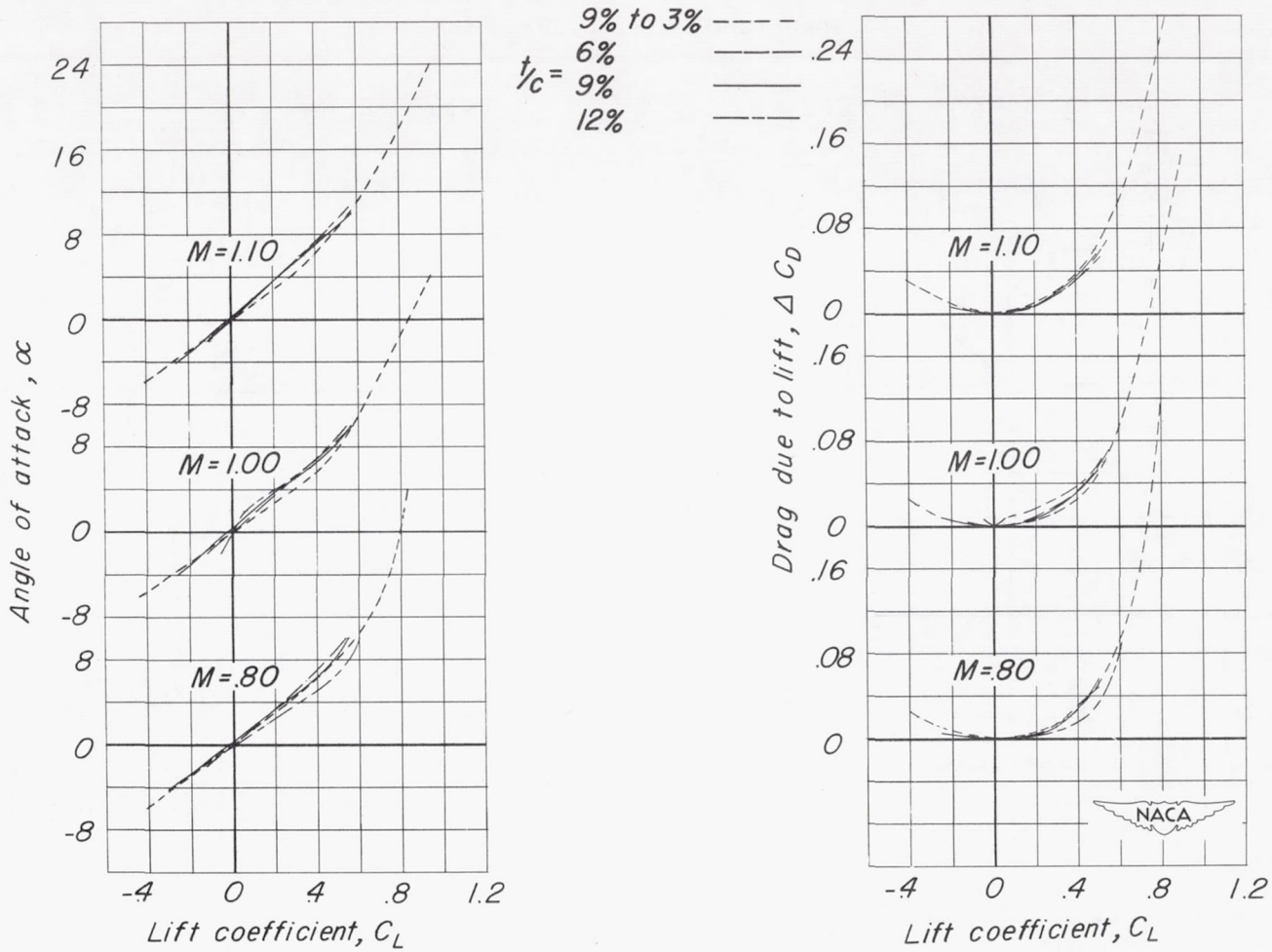

(a) α against C_L.

(b) ΔC_D against C_L.

Figure 11.- Comparisons at representative Mach numbers of the effects of thickness ratio on the aerodynamic characteristics of wings having 45° of sweepback, aspect ratio 6, and taper ratio 0.6.

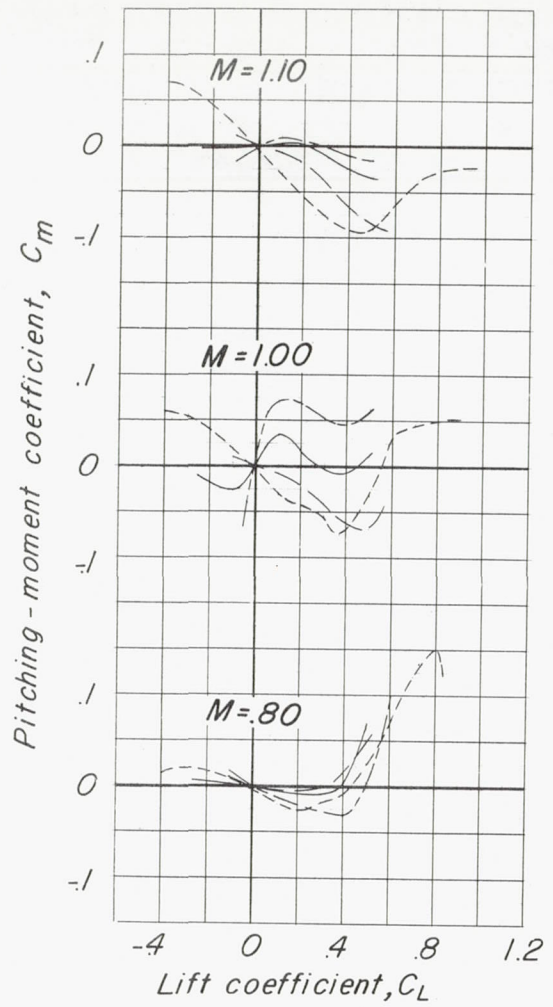

(c) C_m against C_L.

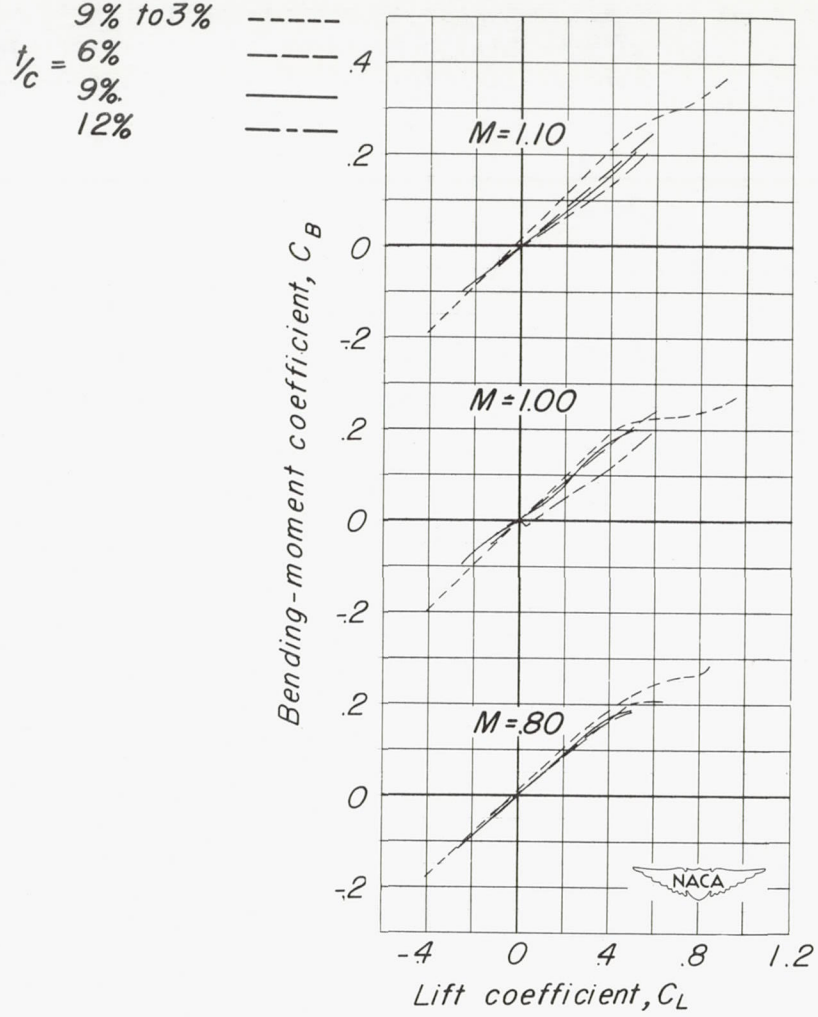

(d) C_B against C_L.

Figure 11.- Concluded.

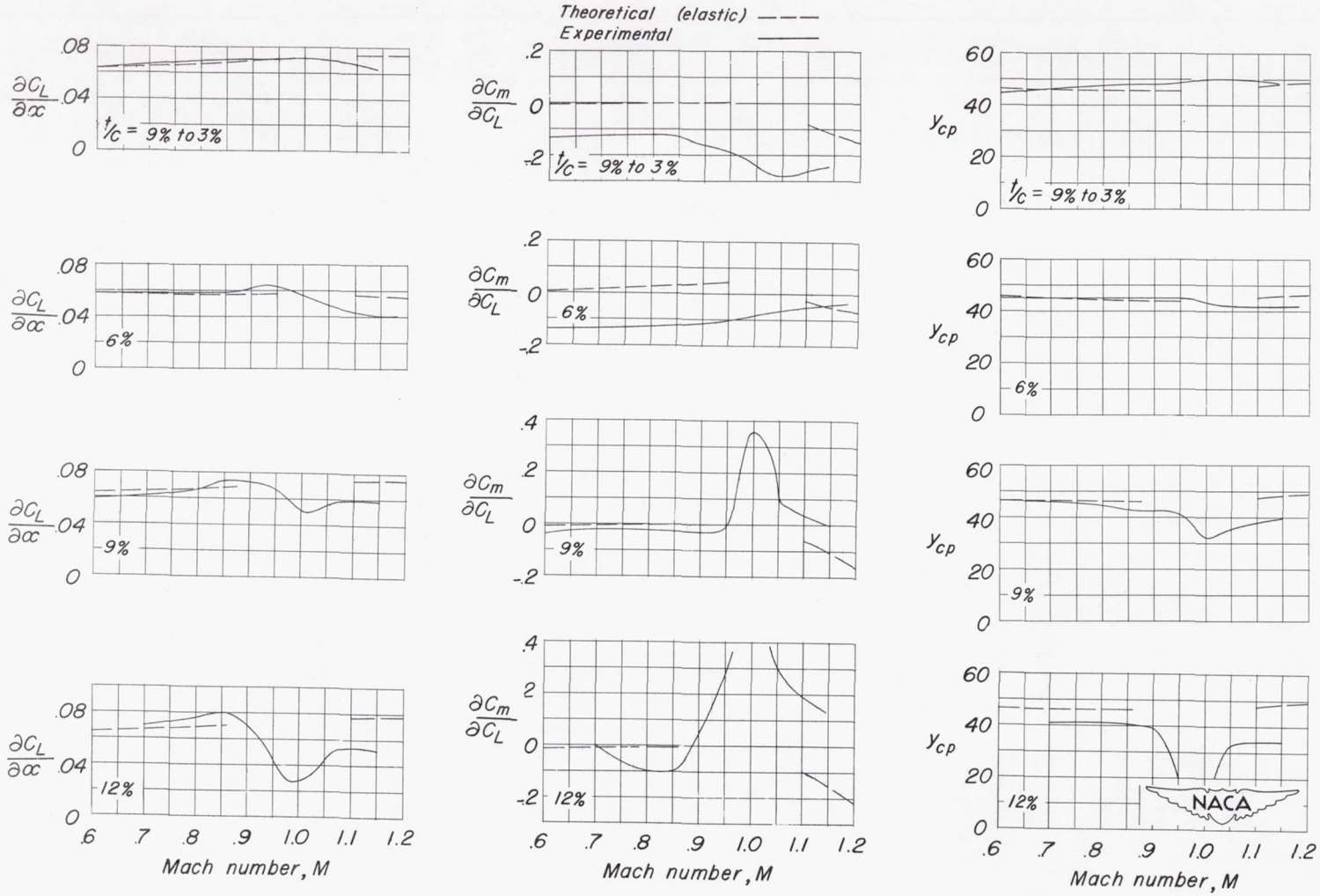

Figure 12.- Theoretical and experimental comparisons of the effects of thickness ratio on the aerodynamic characteristics of wings having 45° of sweepback, aspect ratio 6, and taper ratio 0.6.

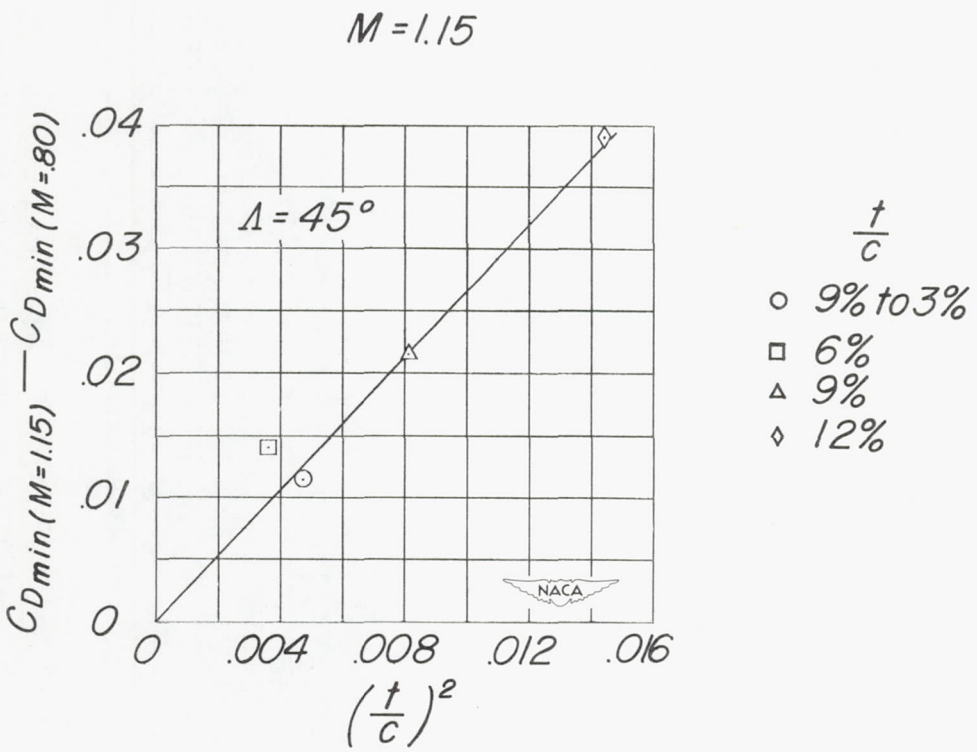

Figure 13.- Pressure drag coefficient against $\left(\frac{t}{c}\right)^2$ at Mach number of 1.15.

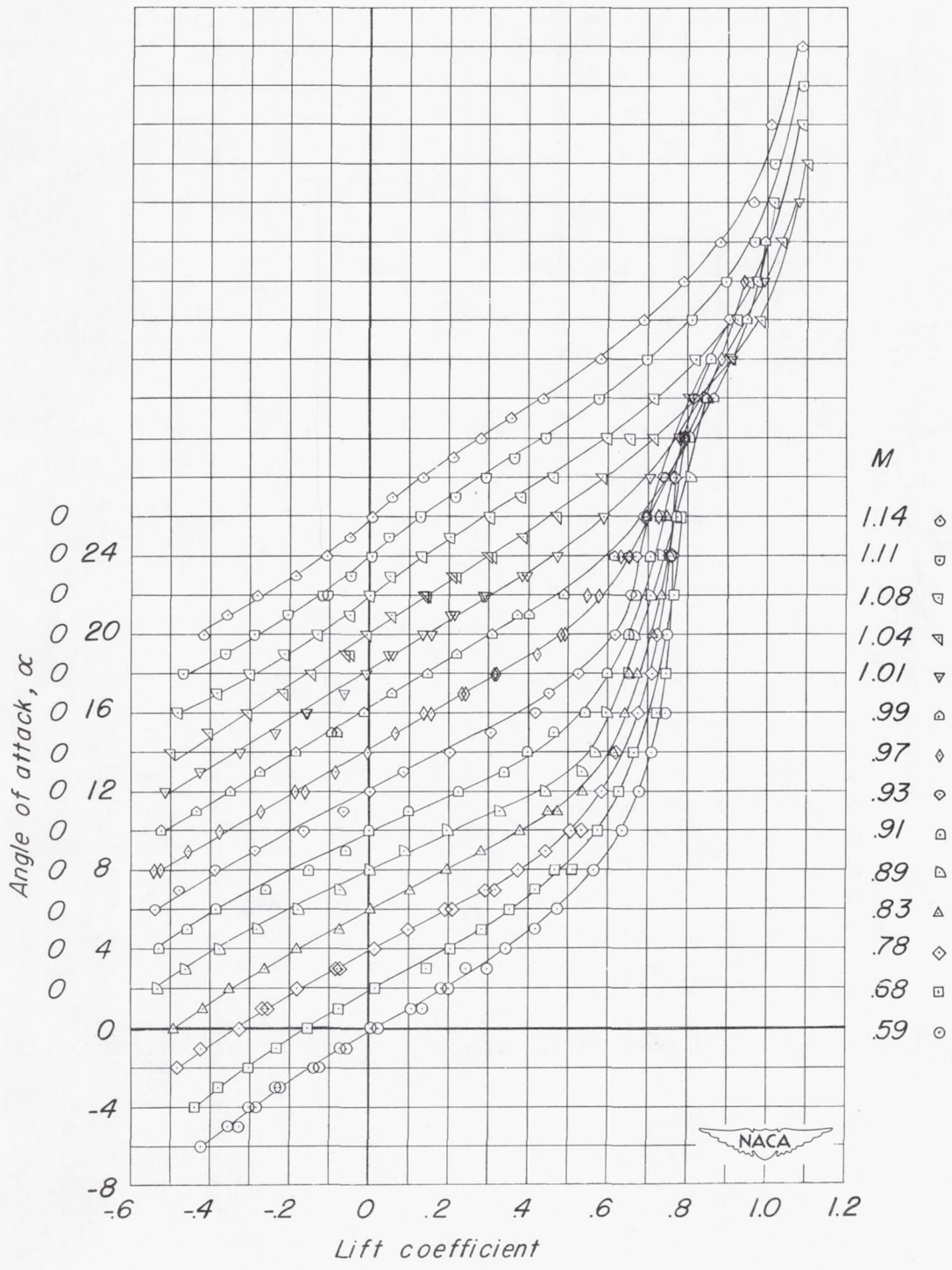

(a) α against C_L.

Figure 14.- Basic aerodynamic data for a wing having 35° of sweepback, aspect ratio 6, taper ratio 0.6, and NACA 65A009 airfoil section at the root chord tapered to NACA 65A003 airfoil section at tip chord.

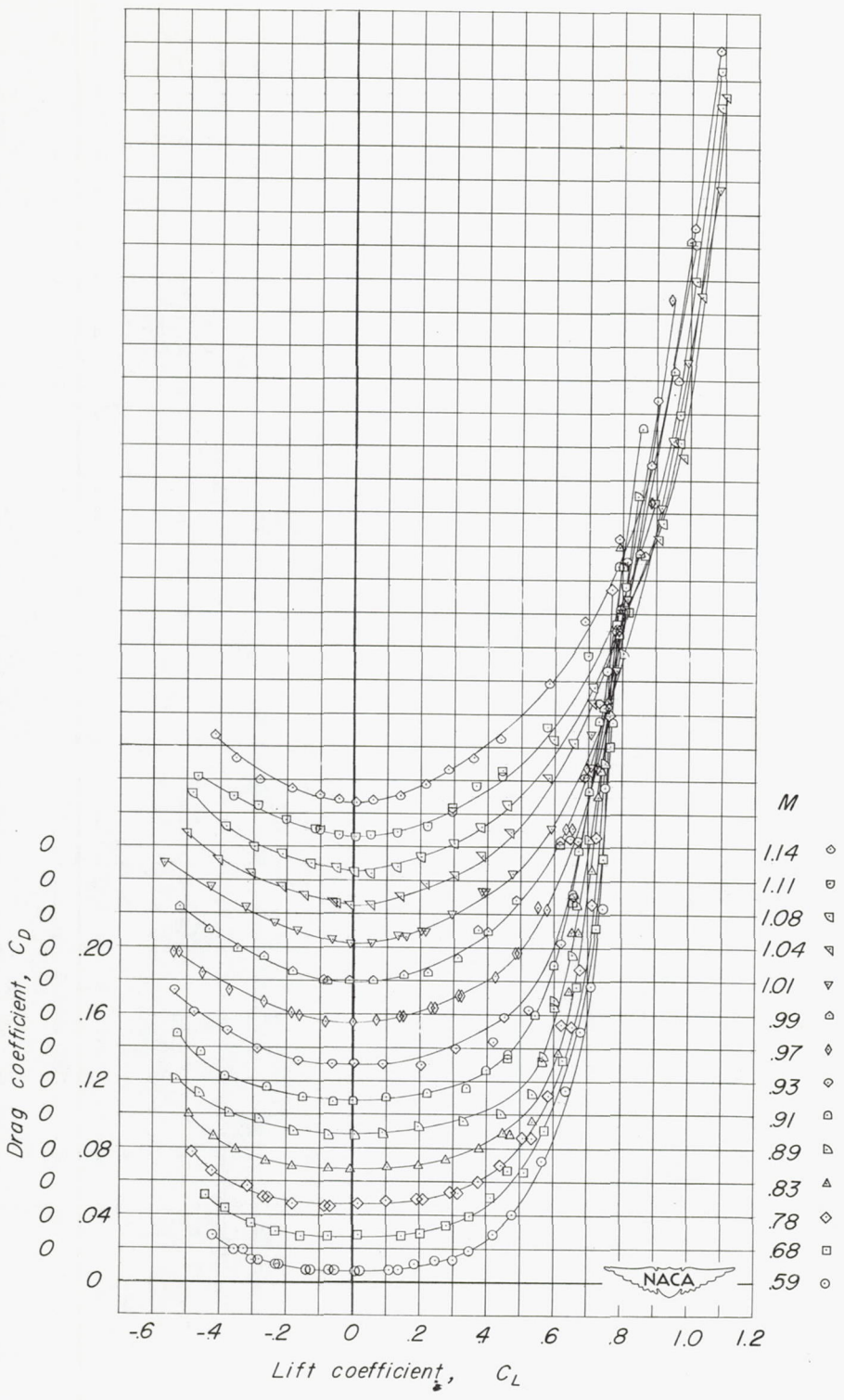

(b) C_D against C_L.

Figure 14.- Continued.

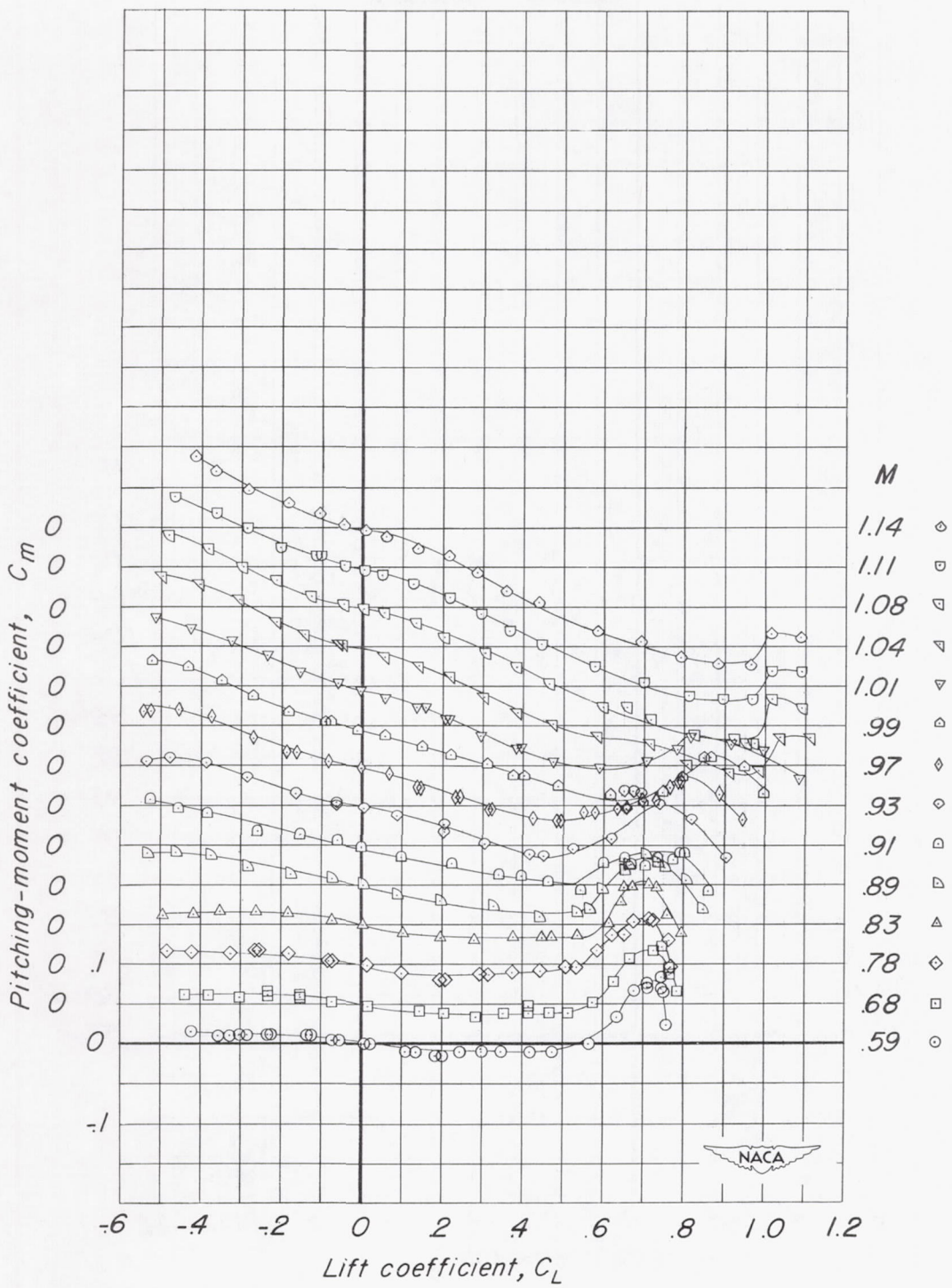

(c) C_m against C_L.

Figure 14.- Continued.

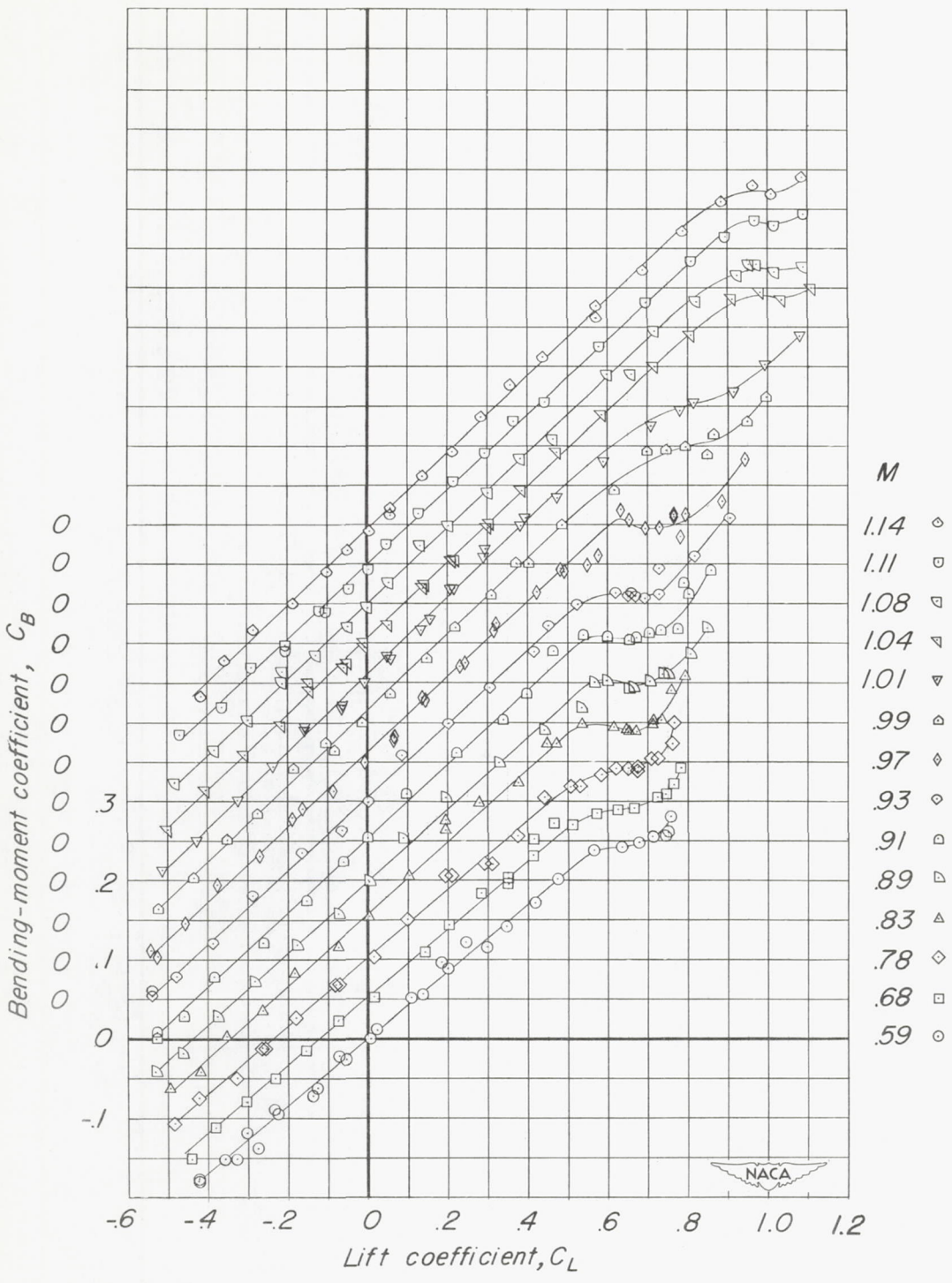

(d) C_B against C_L.

Figure 14.- Concluded.

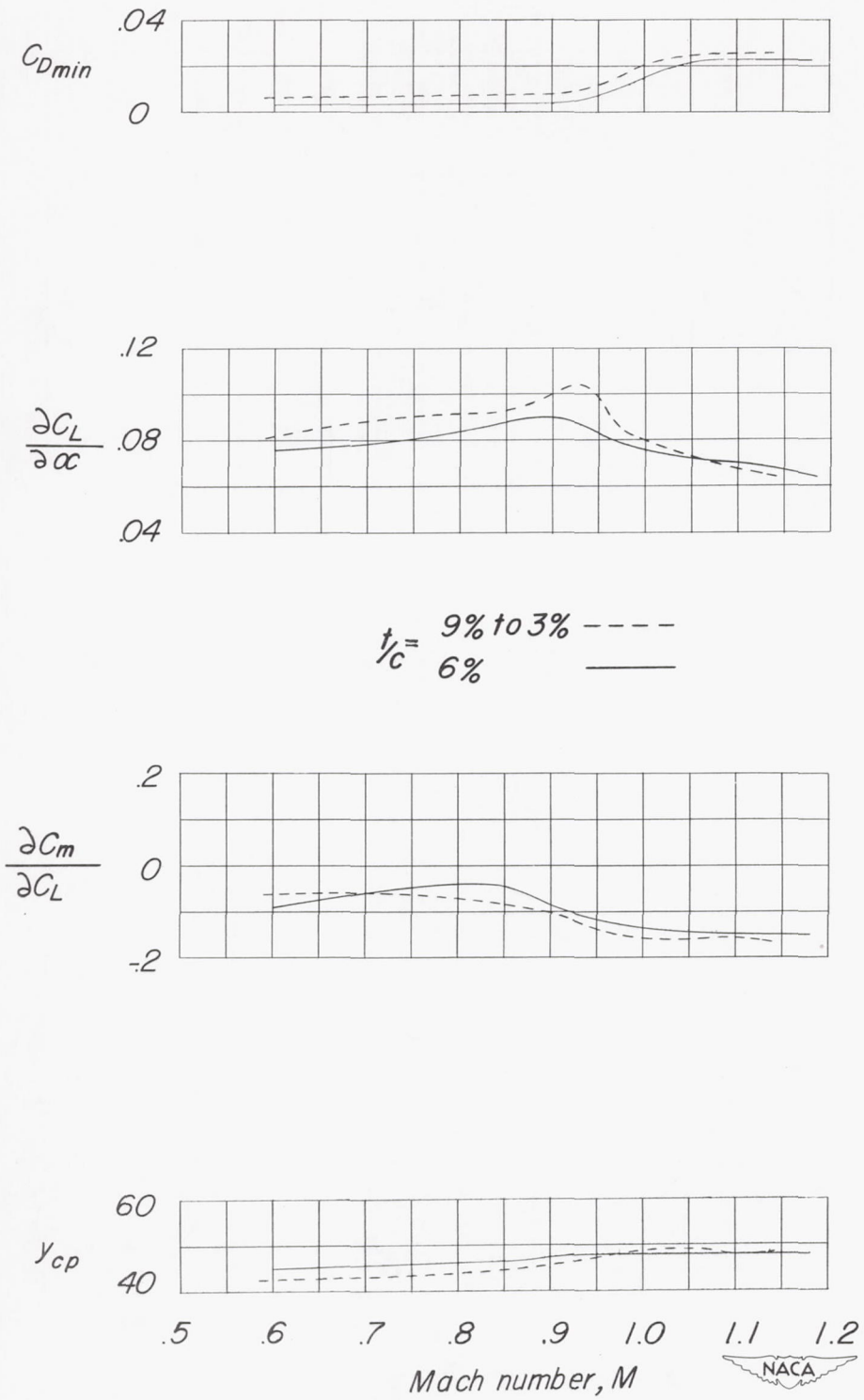

Figure 15.- Comparison of the effects of thickness ratio on the aerodynamic characteristics of wings having 35° of sweepback, aspect ratio 6, and taper ratio 0.6.

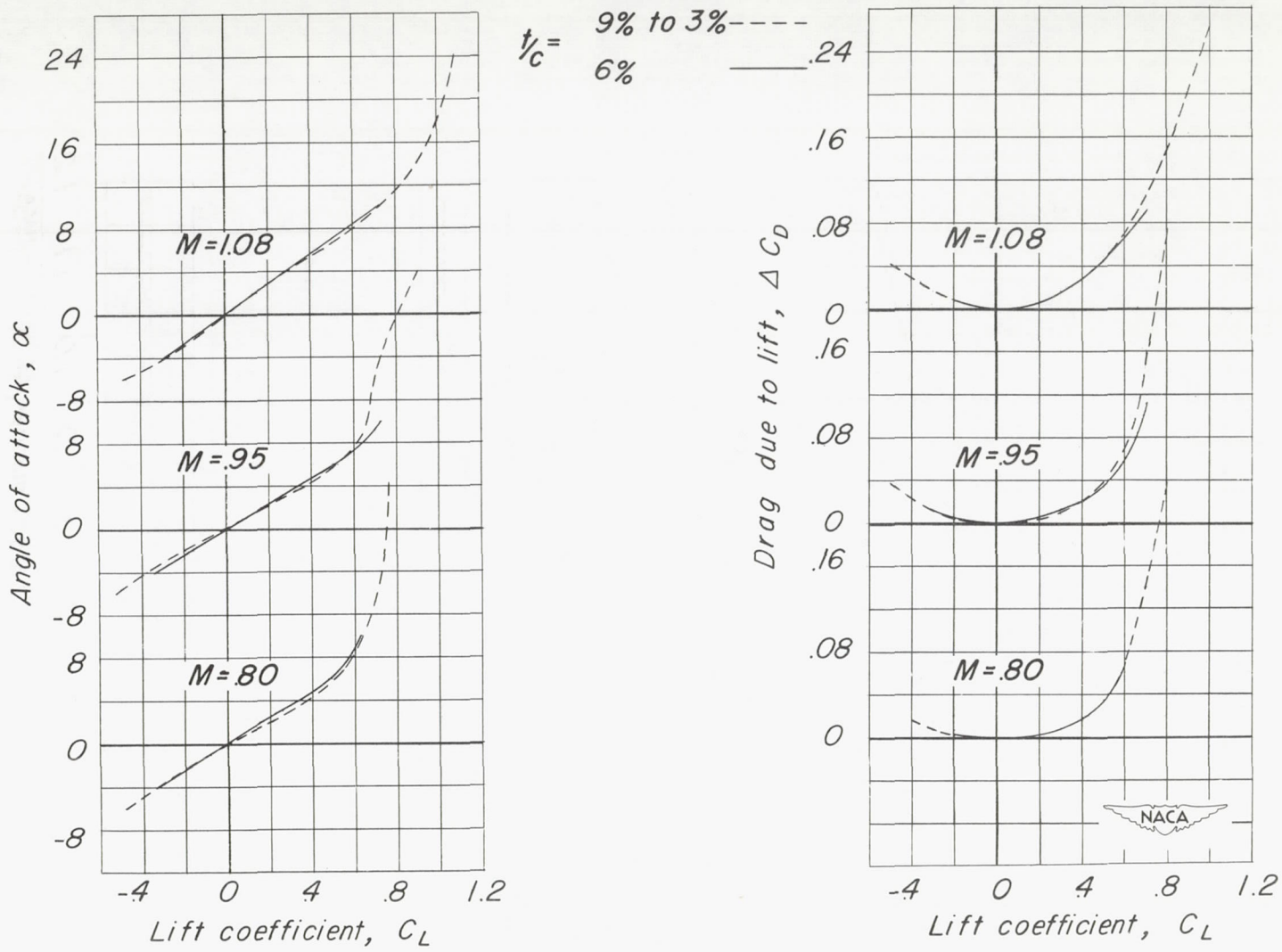

(a) α against C_L. (b) ΔC_D against C_L.

Figure 16.- Comparisons at representative Mach numbers of the effects of thickness ratio on the aerodynamic characteristics of wings having 35° of sweepback, aspect ratio 6, and taper ratio 0.6.

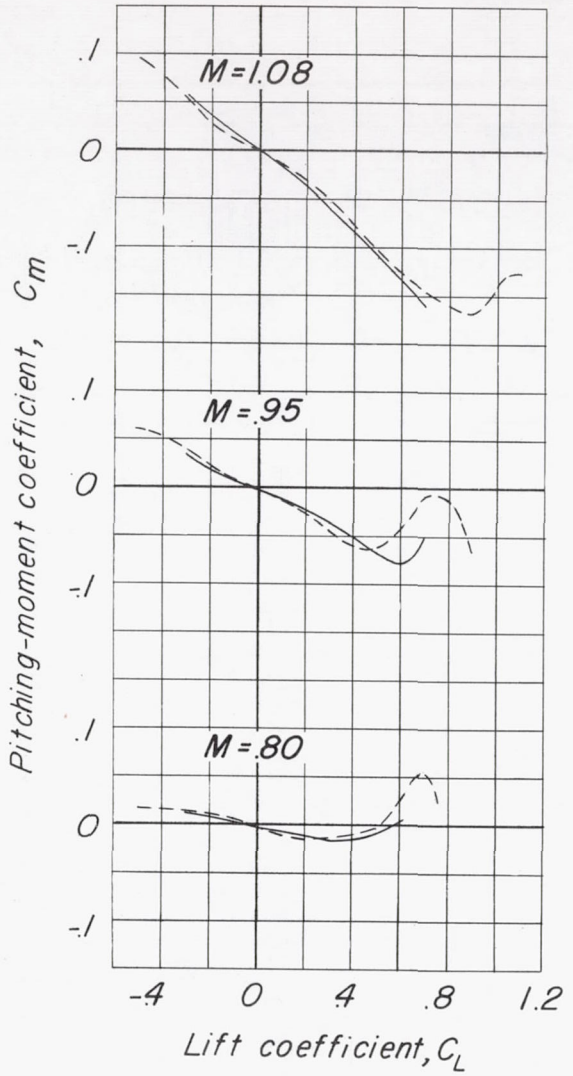

(c) C_m against C_L.

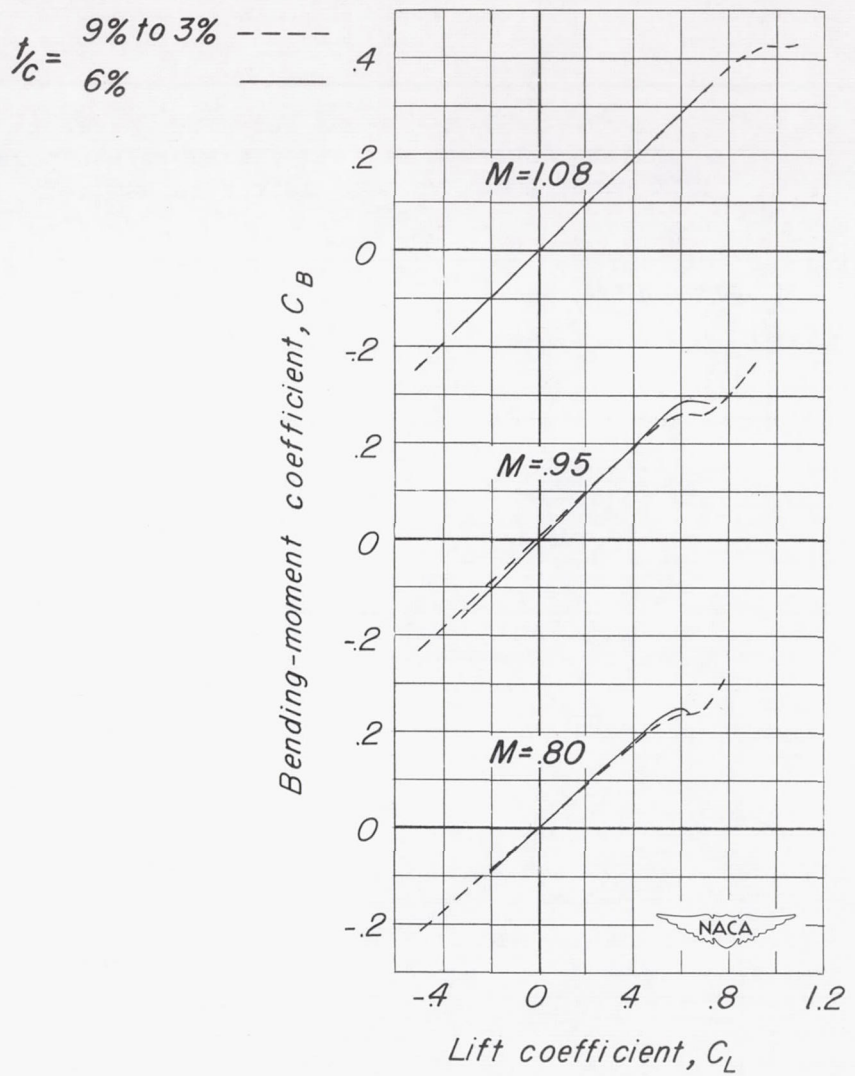

(d) C_B against C_L.

Figure 16.- Concluded.

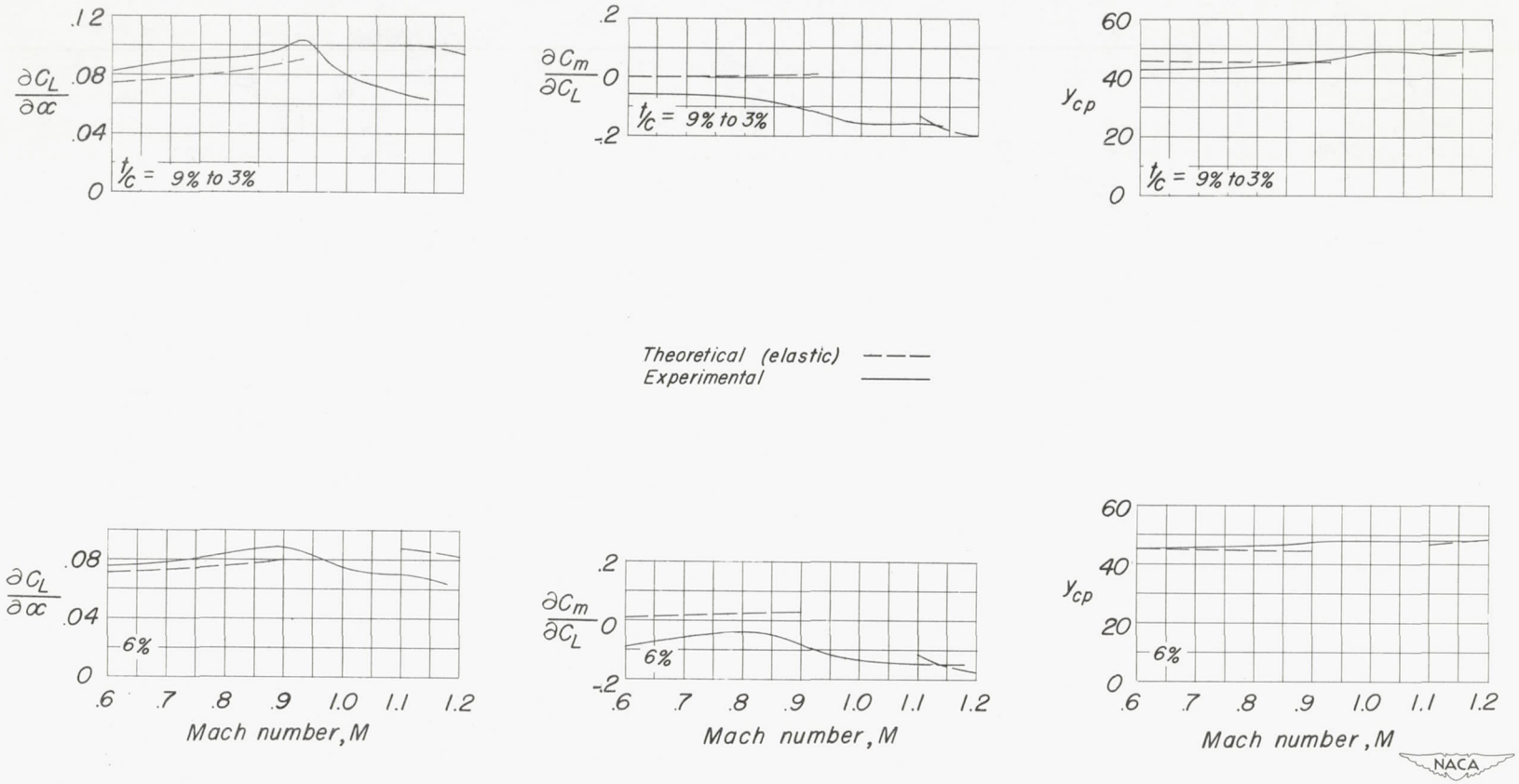

Figure 17.- Theoretical and experimental comparisons of the effects of thickness ratio on the aerodynamic characteristics of wings having 35° of sweepback, aspect ratio 6, and taper ratio 0.6.